Naval Research Laboratory

Washington, DC 20375-5320

NRL/MR/6180--00-8466

Application of CFAST to Shipboard Fire Modeling I. Development of the Fire Specification

J.B. HOOVER
P.A. TATEM

Navy Technology Center for Safety and Survivability
Chemistry Division

June 26, 2000

REPORT DOCUMENTATION PAGE

Form Approved
OMB No. 0704-0188

1. AGENCY USE ONLY (*Leave Blank*)	2. REPORT DATE	3. REPORT TYPE AND DATES COVERED
	June 26, 2000	Interim Report 1998-2000

4. TITLE AND SUBTITLE

Application of CFAST to Shipboard Fire Modeling I. Development of the Fire Specification

5. FUNDING NUMBERS

6. AUTHOR(S)

J.B. Hoover and P.A. Tatem

7. PERFORMING ORGANIZATION NAME(S) AND ADDRESS(ES)

Naval Research Laboratory
Washington, DC 20375-5320

8. PERFORMING ORGANIZATION REPORT NUMBER

NRL/MR/6180--00-8466

9. SPONSORING/MONITORING AGENCY NAME(S) AND ADDRESS(ES)

Office of Naval Research
Arlington, VA 22217-5660

10. SPONSORING/MONITORING AGENCY REPORT NUMBER

11. SUPPLEMENTARY NOTES

12a. DISTRIBUTION/AVAILABILITY STATEMENT

Approved for public release; distribution is unlimited.

12b. DISTRIBUTION CODE

13. ABSTRACT (*Maximum 200 words*)

The use of the Consolidated Fire Growth and Smoke Transport (CFAST) fire model is well established within the civilian community. In recent years, the U.S. Navy has sponsored enhancements to the model (including the addition of vertical vent flow, corridor flow, and improved heat conduction) to make the model more useful in Navy fire scenarios. This report is the first of a series intended to document the current state of CFAST, identify areas in need of further development work, indicate the types of Navy problems which may be addressed by CFAST, and suggest procedures for the routine application of CFAST in ship design.

14. SUBJECT TERMS

Fire modeling
CFAST
Shipboard fires
Fire specification

15. NUMBER OF PAGES

68

16. PRICE CODE

17. SECURITY CLASSIFICATION OF REPORT	18. SECURITY CLASSIFICATION OF THIS PAGE	19. SECURITY CLASSIFICATION OF ABSTRACT	20. LIMITATION OF ABSTRACT
UNCLASSIFIED	UNCLASSIFIED	UNCLASSIFIED	UL

NSN 7540-01-280-5500

Standard Form 298 (Rev. 2-89)
Prescribed by ANSI Std 239-18
298-102

CONTENTS

APPLICATION OF CFAST TO SHIPBOARD FIRE MODELING
I. DEVELOPMENT OF THE FIRE SPECIFICATION

1.0 INTRODUCTION

It is well known that the Navy must reduce shipboard manning requirements while simultaneously maintaining at least the current levels of tolerance to both combat and accidental casualties. Several on-going demonstration projects, such as Damage Control - Automation for Reduced Manning (DC-ARM) and Reduced Ship-Crew by Virtual Presence (RSVP), attempt to address these issues by increasing the use of automation.

The development of advanced damage control modeling techniques supports these efforts by providing improvements in two areas: (a) validation of new ship designs for inherent fire safety; and (b) real-time prediction of fire behavior. In furtherance of these goals, the US Navy has partially funded development, at the National Institute of Standards and Technology (NIST), of the Consolidated Fire Growth and Smoke Transport (CFAST) model [1].

CFAST is already used by the civilian fire protection community to simulate building fires and it has proven useful for building design and post-mortem analysis of fires. The Navy's funding has been directed toward making CFAST more useful for simulation of shipboard fires by adding capabilities for modeling phenomena that are absent from, or of little significance to, building fires. In particular, mass transport through vertical vents (representing hatches and scuttles) [2], energy transport via conduction through decks [3] and an improved radiation transport submodel [4] have been added to CFAST. Work is currently in progress at NIST and the Naval Research Laboratory (NRL) to add (and validate) algorithms for heat conduction through bulkheads.

Fire models can be categorized as field or zone models, depending on the level of spatial detail that they provide. Field models typically divide the region of interest into anywhere from several hundred to several million small volumes (cells), the dimensions of which are typically on the order of centimeters. For each cell, the values of a set of variables are tracked as a function of time. The variables that are calculated include the temperature, pressure and species concentrations. Each variable is represented as a time variant vector field (hence the name field model).

Field models are very slow — it is not unusual to require hours of super computer time to simulate fractions of a second of real time, even for physically small systems. This is partly due to the large number of cells involved, which require a correspondingly large number of calculations, and partly due to the need to use partial differential equations to represent both time and spatial variations.

In contrast, zone models normally use a much smaller number of very large cells (now called zones). For example, it is common to use one or two zones to represent an entire room in a zone model, whereas a field model might use hundreds of thousands of cells for the same volume. Since zones are treated as homogeneous regions, the number of variables that must be calculated is greatly reduced, as compared to a field model. Furthermore, zone models can use ordinary, rather than partial, differential equations because they only need to represent the time variations of the variables. As a result of these differences, zone models can be many orders of magnitude faster than field models.

In the case of CFAST, the model was designed to execute very quickly (in real-time, or better) on affordable desktop computers, which is a requirement for use as a real-time decision aid. In addition, it was intended to be relatively simple to use, which makes the model accessible to users (such as ship architects and shipboard damage control personnel) who are not experienced fire modelers.

Manuscript approved May 30, 2000.

In order to meet these requirements, the CFAST developers made certain simplifying assumptions (in addition to those which are inherent in zone models) regarding the range of phenomena and the types of scenarios which were to be modeled. In turn, these assumptions led to limitations on the scope of the problems which can be modeled, the ease with which they can be modeled and the accuracy of the results. We may categorize these limitations as inherent (things which CFAST is not capable of doing), or practical (things which require *a priori* knowledge which is not likely to be available or which require too much time and effort to be feasible).

In the case of buildings, the assumptions have proven to be reasonably good and the limitations have not been unduly restrictive. However, Naval fire protection problems differ in many critical respects from those found in the civilian world and it is not clear how CFAST's limits may impact the utility of the model for Naval applications. To address this question, the Office of Naval Research has funded a project entitled "Analysis of the CFAST Fire Model Operating Envelope." The project objectives include identifying CFAST limitations, determining their effects on shipboard fire modeling and developing methods for circumventing those problems that have significant adverse affects.

It should be noted that the importance of any given model limitation depends on what we wish to accomplish with the model. For example, as we discuss in detail below, CFAST assumes the user has significant information regarding the time history of the fire. For ship design applications, this is probably not a serious constraint because the designer is interested in general characteristics, rather than behavior during one specific fire. In all probability, many fires, of different types, sizes and locations, will be modeled as part of the design process.

On the other hand, for real-time prediction, this assumption of fore knowledge of the fire history will be a major problem. Here, it is important that the behavior of one specific fire be accurately predicted and, by the nature of the problem, it is impossible to have any knowledge of how the fire will develop - that is, in fact, the very thing that we want the model to predict.

In order to address situations relevant to the Naval environment, we have chosen to use examples from Series 4 of the Submarine Ventilation Doctrine [5] program as a case study The selected tests were conducted aboard the ex-USS SHADWELL during January 1996. The portion of the ship that was used for these tests was modified to represent the forward half of a USS LOS ANGELES (SSN 688) class submarine and, for this reason, the test area is referred to as SHADWELL/688.

The test configuration is shown in Figure 1. We focused on Laundry Room fires because those accounted for most of the tests and because the Laundry Room provided a geometrically simple starting point. In the first phase of the project, only the Laundry Room was modeled; additional spaces were progressively added to the simulation in subsequent phases. As problems were encountered, they were documented and we attempted to develop methods for working around them.

During each phase, the initial intent was to determine which aspects of shipboard fires could or could not be modeled and what approximations had to be made in the process. In order to minimize bias due to foreknowledge of the actual test outcomes, we deliberately choose to ignore most of the test data during this phase. Once these initial goals had been achieved, the resulting model predictions were compared with experiment to determine the accuracy of the various approximation methods.

This report summarizes the results of the first phase, modeling of the fire room, and focuses on the development of the fire specification. In order to understand how the model was built, and

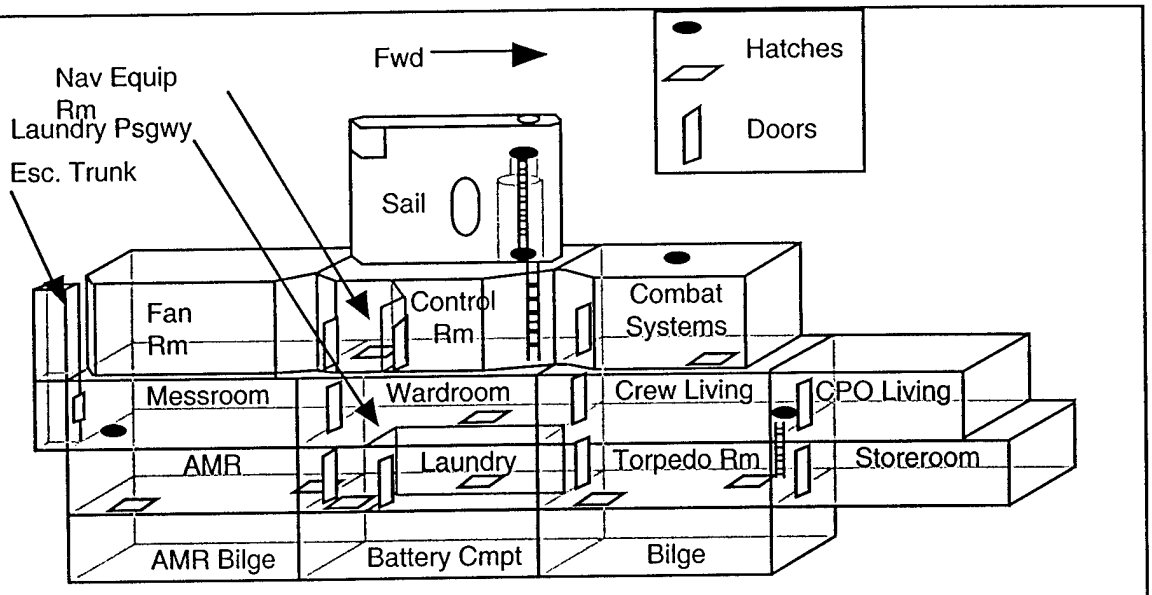

Figure 1. Test Configuration for the Submarine Ventilation Doctrine Test Program

The fires modeled during this study were diesel pan fires, located in the laundry room.

why it was done that way, we first discuss some of the basics of using CFAST. Further details may be found in the CFAST users' guide [6]. We then consider the specifics of the Laundry Room model and compare our model predictions with available experimental results.

2.0 CFAST INPUT REQUIREMENTS

CFAST, like other fire models, requires that the user provide an input file that describes the problem that is to be modeled. This file has a prescribed format that may be likened to the vocabulary of a language. It should be evident that only those scenarios that can be adequately described in this language can be modeled. For this reason, we begin by discussing CFAST's input parameters, which dictate what can, and can not, be described.

2.1 Description of Major CFAST Input Parameters

CFAST inputs are identified by keywords, each of which appears at the beginning of a line and is followed by one or more parameters. Keywords may be included in any order within the command file and, where appropriate, the parameters associated with keywords appearing later in the file will replace values that appeared earlier.

Keywords may be divided into four categories: (1) simulation control; (2) ambient environment; (3) model geometry and (4) fire description. The keywords used in our work are briefly described in Appendix A.

The set of available keywords has evolved over time as new features have been added. We note that the description that follows is based on CFAST version 3.1.4, which was the current version at the time that this project was started[1]. All of these simulations were run using this version. For reference, input file fragments are included in the following sections. Lines beginning with the pound sign (#) are comments which are ignored by CFAST.

1 Version 4 has been under development at NIST but, as of the date of this report, has not been released for public use.

2.1.1 Simulation control keywords

Parameters in the simulation control category affect the manner in which the fire simulation is executed. They include the model version (VERSN), simulation time (TIMES), the name of the output data file (DUMPR), the time base for events (FTIME) and whether the simulation is to be restarted from the results of a previous run (RESTR). An example of the use of these keywords is given in Listing 1.

```
VERSN    3Test - Two small compartments (no connections)
#       Sim.time  Print  Hist.  Disp.  Copies
TIMES     270      1      1      0      0
DUMPR TWOSMALL.HI
#           t0     t1     t2     t3
FTIME               19.    20.    270.
RESTR PARTONE.HI 19
```

Listing 1. Examples of the CFAST Simulation Control Keywords.

VERSN indicates the version of CFAST for which the file was created and provides an option for labeling the current simulation. TIMES sets the total simulation time, the interval between on-screen printouts and the interval between dumps to the history file, all in seconds. The last two parameters are the interval between graph updates (in seconds) and the number of hard copies of each graph which should be produced. DUMPR specifies the name for the history file and FTIME defines the times at which events occur. The RESTR keyword indicates that the current simulation will be initialized to the conditions that existed 19 seconds into the simulation that was saved as PARTONE.HI.

FTIME deserves further explanation. CFAST allows the user to define events, such as the opening or closing of vents, which can occur at specified times. However, there is only a single time base that is used by all such events. There must be an entry in this time base (in seconds elapsed since the start of the simulation) for each event and, for each event, there must be an entry corresponding to each entry in the time base. In addition to controlling the opening and closing of vents, the time line also is used to control the growth of the fire and for other purposes, as is discussed below.

FTIME		t1	t2	t3
CVENT A	0	1	0	0
CVENT B	1	1	1	0

Table 1. Example of the CFAST Event Mechanism

Events can be triggered at the elapsed times (in seconds) specified by FTIME. In this case, the CVENT commands cause vents A and B to fully open (1) or completely close (0) at times zero, t_1, t_2 and t_3. Note that an event time at zero seconds is implied.

For example, suppose we wish to specify that vent A is initially closed, is open at time t_1 and closed again at time t_2. Furthermore, we want vent B to be initially open and to be closed at t_3. This vent sequence is illustrated in Table 1. We first specify times t_1 through t_3 using the FTIME

keyword. We then specify each of the vent openings (as a fraction of the maximum width[2]) for each of the times, even if there is no change for that vent at that time. Note that there is an implicit t_0 in FTIME but events must be explicitly provided for all times, including t_0 (*i.e.*, the first event in each set is assumed to occur at t_0, even though zero is not listed in the time line). This is because CFAST reads the events from left to right; the first event is assumed to occur at zero time and subsequent events are sequentially associated with the times listed in the FTIME line. If an event is missing, then the following events will be associated with the wrong time. CFAST uses linear interpolation to calculate values for intermediate times, as shown in Figure 2.

The event mechanism may also be used to alter some aspects of the fire, such as the fire size, during the simulation. In general, step function changes cause CFAST to fail (because the equation solver can not converge) so changes should be defined to occur over a period of several seconds. Step changes can be introduced, if necessary, by using RESTR to initialize the simulation to values calculated by a previous simulation. This is particularly useful when there is a sudden change in the type of fuel involved. For example, some of the NRL large-scale tests began with hexane pan fires and switched, virtually instantaneously, to a diesel spray fire. This was modeled by first simulating the pan fire, using parameters characteristic of hexane, up to the time of ignition of the spray fire and then restarting the model with different fire parameters.

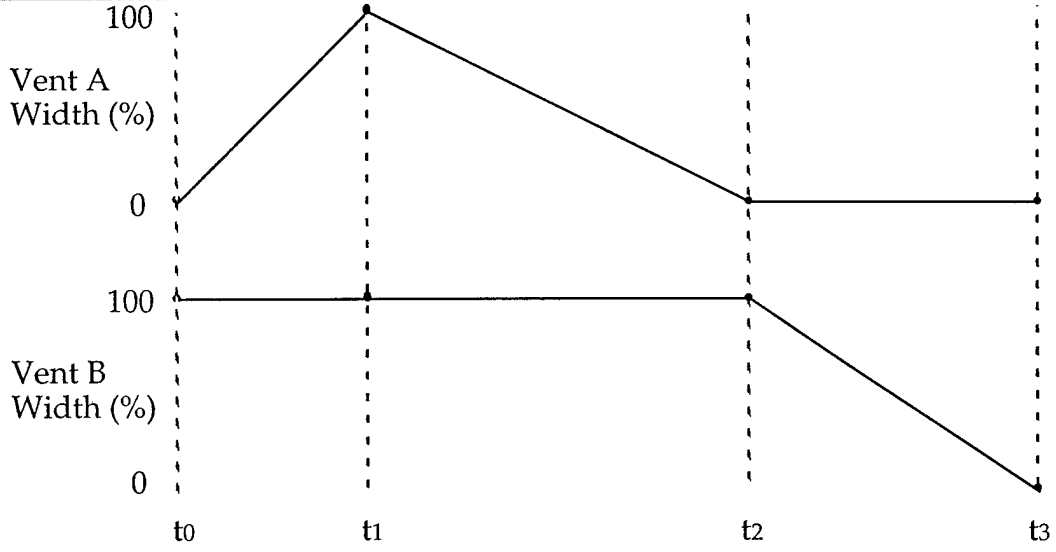

Figure 2. Example Vent Widths

The widths of Vents A and B, as defined in Table 1, are shown for all simulation times between t0 and t3. Note that widths at intermediate times are interpolated from the values at the specified times.

2.1.2 Ambient condition keywords

Listing 2 illustrates the use of the two ambient environment keywords, TAMB and EAMB. The former indicates the initial conditions within the simulation region; the latter refers to the exterior conditions. There can only be one instance of each. Note that the requirement that there be only a single TAMB line implies that the entire model domain is assumed to be described by the same initial condition prior to the start of the simulation.

[2] CFAST only permits vent widths to be varied. This is appropriate for doors but does not correctly represent vertically opening vents such as windows.

```
#     Temp        Pressure     Ref. Elev.
TAMB  300.000     101300.      0.000000
EAMB  300.000     101300.      0.000000
```

Listing 2. Examples of the CFAST Ambient Condition Keywords.

TAMB and EAMB describe the initial temperature and pressure and reference elevation within and outside of the modeling domain, respectively. The reference elevations are the actual elevations (meters) at which the temperatures and pressures were specified.

For each keyword, the temperature, pressure and reference elevation are given. The elevation of the reference point is needed so that the model can correct for altitude-related temperature and pressure changes. Correction for differences in elevation can be important for high-rise buildings, but is not expected to be significant for shipboard fire modeling. The same reference point must be used for both keywords.

2.1.3 Geometry keywords

The dimensions of each compartment are specified using DEPTH, WIDTH and HEIGH and the compartment's floor elevation, relative to the reference point defined by the ambient environment inputs, is given by HI/F. The requirement that the compartment dimensions be completely specified by three values means that each compartment must be a rectangular parallelepiped. This imposes an implicit restriction on the range of geometry that can be modeled by CFAST.

Construction materials used for the ceiling, walls and floor are identified by the keywords CEILI, WALLS and FLOOR, respectively. The parameters for these keywords are the names of the construction materials, as they appear in the material property database, which is a text file. By default, the file THERMAL.DF is used, but this can be changed to another file by using the THRMF keyword. The properties database contains the name of the material and a list of thermophysical properties, which include thermal conductivity, specific heat, density, thickness and emissivity. The term "thermophysical properties database" is somewhat misleading because the values apply to a specific thickness of the material. Thus, the database we used included many entries for steel, reflecting the different thicknesses used in various parts of the SHADWELL.

Note also that only one material (including thickness) can be defined for the ceiling, walls or floor of any given compartment. If any boundary of the compartment in question has regions constructed of different materials (or different thicknesses of the same material), then some approximation must be applied. Finally, CFAST considers walls to be wrap-around entities — each compartment is treated as if it were surrounded by a single wall, not by four separate walls. It follows that it is not possible to exactly model situations where the different walls are composed of different materials — some approximations must be made in this case.

Each of the keywords mentioned above (except for THRMF) is followed by a list of values, one value per compartment. Compartment numbers are determined by the order of the parameters, *i.e.,* the first parameter following the keyword applies to compartment one, the next to compartment two and so on. There is no keyword to declare the number of compartments; instead, CFAST determines this value by counting the parameters associated with these keywords. If N parameters are found, CFAST assumes there are N compartments. Furthermore, it also assumes that "compartment" (N+1) refers to the world outside of the model domain. If different numbers of parameters appear on different lines of the input file, CFAST will run without reporting any errors but the results, as might be expected, are likely to be erroneous.

HVENT and VVENT are used to define horizontal and vertical vents, respectively. In CFAST terminology, a vent is almost any opening between compartments (or between a compartment and the outside), except for ventilation ducts, which have their own special set of keywords. Since we did not use ventilation ducts in this model, references to vents appearing in this report refer to doors, windows, hatches, scuttles and similar openings. Another oddity of CFAST nomenclature is that vents are described by the direction of the flow through the vent, not by the orientation of the vent itself. For example, a door is a horizontal vent, because it allows horizontal flow, although the orientation of the door is vertical.

HVENT requires six parameters and there are three, seldom used, optional parameters. The first two required parameters identify the two compartments that are connected by the vent. As mentioned above, compartment numbers are determined by the order in which their dimensions were declared. Recall that, for an N-compartment simulation, compartment (N+1) represents the ambient environment. This convention allows the definition of vents that connect between a real compartment and the external environment.

CFAST permits up to four HVENTs between the same pair of compartments, so the third HVENT parameter is a number (from one to four) which identifies which particular vent is being defined. The next three parameters specify the vent width, the height of the soffit (top) and the height of sill (bottom), respectively. The optional parameters will not be discussed here since they were not used in our work.

Like HVENT, VVENT also requires two parameters to define the connected compartments. In addition, the area of the vent must be given and the shape is specified as either circular or square. Vents of other shapes must be replaced by equivalent round or square openings. Note that "equivalent" refers to the flow resistance of the vent and not to the actual vent area.

The CVENT keyword permits specification of horizontal vent closure events. The CVENT parameters are the compartment numbers and the vent identification number, as defined by HVENT, and a list of fractional vent openings. As was illustrated in Table 1, the first fraction refers to the vent opening at zero time and subsequent entries correspond to successive event times, as established by FTIME. CVENT was not used in the present work because, in the SHADWELL tests selected for modeling, none of the vent openings was changed. At present, it is not possible to define closure events for vertical vents.

The last keyword in this category is CFCON, which is used to enable vertical heat conduction through a ceiling/floor from the lower compartment to the upper. In the absence of this keyword, CFAST calculates outward heat conduction through the ceiling of the lower compartment, but does not include this energy as a heat source for the upper. This keyword was not needed for the first modeling phase because there was no upper compartment. It is expected that it will be an

important factor in later phases that do include compartments on multiple decks. At present, there is no corresponding horizontal conduction keyword, but this feature is under development at NIST.

The use of most of these keywords is shown in Listing 3. Since this example did not have vertically stacked compartments, CFCON was not used. Also, the default materials property database, THERMAL.DF, was used so there was no need for the THERMAL keyword.

2.1.4 The need for a fire specification

The CFAST model uses a specified, rather than a self-consistent fire. This means that the user must provide a time-dependent description of the growth of the fire. In contrast, with a self-

consistent fire, only details of the initial fuel load and geometry would be given and the model would then predict the fire size at later times.

```
#       Cmpt. 1  Cmpt.2
DEPTH   4.00000  4.00000
WIDTH   4.25000  4.25000
HEIGH   2.60000  2.60000
HI/F    0.00000  0.00000
CEILI   SHIP3/8  SHIP3/8
WALLS   SHIP2/8  SHIP2/8
FLOOR   SHIP3/8  SHIP3/8
#       Cmpt.1   Cmpt.2  Vent #  Width    Soffit   Sill   Wind
HVENT   1        3       1       1.000    2.100    0.000  0.000
#       Cmpt.1   Cmpt.#  Vent#   <--------Width Fraction-------->
CVENT   1        3       1       1.000    1.000    1.000    1.000
```

Listing 3. Examples of the CFAST Geometry Keywords.

These are the major keywords used to define the geometry for a CFAST simulation. The first three specify the dimensions of the compartments, HI/F is the compartment floor height (relative to the reference elevation from Listing 2) and the next three lines identify the materials used. The actual properties of these materials are contained in a separate database file, THERMAL.DF. HVENT specifies horizontal vents (doors, for example) while CVENT permits vents to be opened or closed during the simulation. Note that, since there are only two compartments defined, compartment three represents the external environment rather than a real compartment.

We should note that referring to CFAST as a fire model is somewhat misleading: CFAST models the effects of the fire but does not actually model the fire itself. Fires involve an extremely complex set of interacting chemical reactions and any attempt to model them would require detailed information regarding the thermodynamics and kinetics of those reactions. More fundamentally, it would require the use of a field model, which would defeat the purposes of CFAST. Rather than simulate chemical reactions, CFAST uses user-supplied ratios to estimate the relative concentrations of various combustion products for a given quantity of burned fuel. The amount of fuel consumed is based on the user-specified fire growth description.

This requirement for a specified fire is probably the most important restriction on the use of CFAST. As will be seen in the next section, there are a relatively large number of parameters involved in the fire specification and considerable effort must be expended to ensure that the description is internally consistent. Furthermore, even more work is required to verify that the specified fire matches a specific real fire if, as in the present work, that is the goal of the simulation.

It is known that, for most "normal" fires (*i.e.*, those that do not involve explosions) the heat release rate of the fire is the most important single predictor of the hazard posed by the fire [7]. Therefore, we expect that the input heat release rate will be critical to achieving accurate model predictions of temperature. If accurate prediction of oxygen or toxic gas concentrations is also needed, then a host of other parameters involving combustion chemistry factors will also be important.

Prediction of temperatures was the primary focus of this work, with carbon dioxide and oxygen concentrations second and carbon monoxide and soot (obscuration) last. This order was dictated primarily by the availability of data for eventual comparison with the model — the Submarine

Ventilation Doctrine tests produced a large amount of temperature data, a much smaller amount of gas concentration data and almost no soot data.

The fire specification outlined above applies to the so-called main fire. This fire is assumed to ignite at time zero and then burns in accordance with the specification. In addition to the main fire, CFAST provides a capability for specifying object fires. These are intended to represent real objects, such as furniture, which are assumed to be ignited at a specified time, surface temperature or surface heat flux. Object fires were not used in our work and will not be discussed further.

2.1.5 Fire specification keywords

Listing 4 provides examples of the use of fire specification keywords. The location of the main fire is given by LFBO and FPOS. LFBO takes, as a parameter, the number of the compartment in which the fire is located; FPOS specifies the coordinates of the fire within that compartment. FPOS uses a right-handed Cartesian coordinate system with the origin at the lower, left, rear corner of the room.

```
#       Fire Cmpt
LFBO    1
#      X       Y       Z
FPOS   2.000   2.125   0.000
#      Fire Type (1 = unconstrained; 2 = constrained)
LFBT   2
#                      19.          20.              270.
FQDOT       0.000      0.000        1.800E+006       1.800E+006
#        Mol Wt    Rel Hum    LOL      Hc          Init T    Ign. T    Rad. fract.
CHEMI    16.       0.000      5.0      5.0E+7      300.      600.      0.000
#                      19.          20.          270.
HCR          0.333     0.333        0. 333       0.333
O2           0.000     0.000        0.000        0.000
OD           0.000     0.000        0.000        0.000
CO           0.000     0.000        0.000        0.000
HCN          0.000     0.000        0.000        0.000
HCL          0.000     0.000        0.000        0.000
CT           0.000     0.000        0.000        0.000
CJET OFF
```

Listing 4. Examples of the CFAST Fire Specification Keywords.

This fire is located in compartment one at the coordinates given in FPOS. It is a constrained (type 2) fire which ignites at 19 seconds and reaches 1.8 MW in one second. Since FQDOT and ΔH_c are explicitly declared, there is no need for FMASS. CHEMI, HCR, O2, CO, HCN, HCL and specific parameter values which are reasonable for a lean methane fire. FHIGH is not used since the base of the fire does not change in this example. CJET OFF invokes the standard convection algorithms.

Fires may be defined as either unconstrained (type one) or constrained (type two) by using the LFBT keyword. These types define the way in which the fire will respond to reductions in atmospheric oxygen concentration. In an unconstrained fire, CFAST always uses the specified heat release rate; for a constrained fire, the heat release rate will be reduced below the user-specified level if there is insufficient oxygen to support that combustion rate. We should also note that, for the unconstrained fire, CFAST does not calculate any species concentrations.

The heat release rate of the fire is defined by the interaction of three different keywords: FQDOT, FMASS and CHEMI. FQDOT provides a set of actual heat release rates for the specified event time line. As usual, the first FQDOT value applies to zero time; the remaining values correspond to the event times given in FTIME. FMASS is the pyrolysis (mass loss) rate of the fuel for the same event times and one of the parameters included in the CHEMI line is the heat of combustion, ΔH_c. Since, at any time, the heat release rate is given by

$$dQ/dt = \Delta H_c \, dm/dt \qquad \text{Eqn. 1}$$

where dQ/dt is the heat release rate and dm/dt is the mass loss rate.

it is evident that the fire is over-specified if all three parameters are given. CFAST requires only two of the three and, if all three are present, uses only the last two. For example, if a user includes the three keywords in the order FQDOT, FMASS and CHEMI, the FQDOT inputs will be replaced with new values calculated with Equation 1.

In addition to the heat of combustion, other CHEMI parameters are the molecular weight of the fuel, the initial relative humidity, the lower oxygen limit (LOL) of the fuel vapor, the initial fuel temperature, the fuel vapor ignition temperature and the radiative fraction. The significance of some of these parameters requires further explanation.

Natural concentrations of most atmospheric gases, such as oxygen, carbon dioxide and carbon monoxide, are relatively constant, regardless of location, season or weather conditions. However, water vapor concentration is highly variable so CFAST needs to be told what initial concentration to use. The relative humidity is used to calculate this initial value, which is then modified by the water contribution from combustion. Because water vapor is a strong absorber of infrared radiation, its concentration affects radiation transport and, therefore, temperatures. In addition, humidity is a factor in the calculation of HCl deposition rates.

The lower oxygen limit (LOL) specifies an oxygen concentration (in volume percent) below which the fire will be extinguished. This limit is enforced only for the case of a type two (constrained) fire. As was mentioned in the discussion of the LFBT parameter, CFAST does not calculate oxygen concentrations for unconstrained fires.

The LOL suppression effect is implemented [1] by calculating a combustion factor

$$Fc = 0.5 * \{\tanh [800 (YO - YLOL) - 4] + 1\} \qquad \text{Eqn. 2}$$

where YO is the predicted oxygen mass fraction and YLOL is the oxygen mass fraction at the specified LOL value[3]. This function is very narrow, varying from zero (extinguishment) at the LOL up to one (no suppression) at LOL + 0.01. The default value for LOL, 10%, is based on experiments by Morehart, *et. al.* [8].

The ratio of the radiated energy to the total energy produced during combustion is known as the radiative fraction. The energy generated can either heat the combustion product plume or, by radiation, it can heat the surrounding region. Thus, the radiative fraction is important because it strongly affects the relative temperatures of the gas layers, the walls, floor and ceiling.

[3] Note that LOL is specified in units of volume percent but the calculation is performed in mass fraction units.

There are seven other keywords, in addition to CHEMI, that affect the chemistry of the combustion process: HCR, O2, OD, CO, HCN, HCL and CT,[4]. The first two of these are related to the fuel composition, the next three to the behavior of the fuel during pyrolysis and the last two to the combustion process. Collectively, these keywords provide the information used by CFAST to calculate the production of various pyrolysis and combustion products; the concentrations of these products are then tracked as they spread through the simulated system. The parameters associated with all of these keywords are treated as events so it is possible to specify fires in which the effective chemistry changes with time.

HCR and O2 are the hydrogen-to-carbon and oxygen-to-carbon mass ratios of the fuel, respectively. HCR is used to determine the amount of water vapor produced when the fuel is burned and O2 reflects the amount of oxidizer, if any, that is incorporated into the fuel. Any oxygen provided within the fuel itself reduces the need for atmospheric oxygen and therefore affects the heat release rate and oxygen consumption in constrained fires.

The O2 keyword applies only to special cases, such as that of rocket fuels. Fuels which contain oxygen within the molecular formula may be considered to be partially pre-oxidized (methanol can be thought of as partially oxidized methane, for example). In these cases, the effects of the oxygen are automatically accounted for by the heat of combustion and the O2 keyword is not needed.

HCN and HCL specify the ratios of the masses of hydrogen cyanide and hydrochloric acid in the pyrolyzate to the mass of pyrolyzed fuel. Note that, unlike the previous two keywords, these properties are not intrinsic to the fuel — they can vary in response to changing combustion conditions. However, CFAST can not account for this variation and will always calculate the composition of the pyrolysis products based on these user inputs.

CT is similar to HCN and HCL in that it controls the rate of production of a pyrolysis product and this product is tracked as it spreads through the system. However, CT is not a real product, rather, it is a quantity which represents (based on empirical correlation functions) the total toxic hazard of the actual products. It takes into account the typical toxic effects of such things as carbon monoxide, acid gases and oxygen depletion. The CT input affects the predicted concentration of "total toxics" but does not affect the predictions of temperature or any of the real fire products. Since we were not interested in this "virtual" product, CT was always set to zero in our simulations.

The last two keywords, OD and CO, again specify mass ratios for products, but this time the ratios are calculated with respect to the mass of carbon dioxide in the product, rather than to the mass of some reactant. OD is the soot-to-carbon dioxide ratio and CO is the carbon monoxide-to-carbon dioxide ratio. OD strongly affects the predicted concentration of soot, of course, but also has a major indirect effect on temperatures because soot is the dominant term in calculating radiative energy transport. This effect will be discussed in more detail below.

The OD and CO ratios are variable and, as was the case with the pyrolysis parameters, the user is responsible for providing physically reasonable values. This can be difficult for two reasons: (1) the parameters are ratios of products and any change in the combustion process that affects one product is likely to affect the other, making it difficult to intuitively estimate the net effect on the ratio; and (2) due to sensitivity to the combustion conditions, it is often not possible to find literature values appropriate to the simulation conditions. Furthermore, even if values consistent

[4] In common usage, OD refers to optical density while CO and O2 refer to the species carbon monoxide and oxygen, respectively. CFAST assigns different meanings to these terms and this non-standard usage sometimes causes confusion. In this report, OD, CO and O2 are always used in the CFAST sense and species are spelled out.

with the expected conditions are specified, the conditions calculated by the model may be very different from the user's expectations.

For example, suppose that you anticipate that the fire will always be well ventilated and specify an OD value that is appropriate for this case. If the model predicts some unanticipated ventilation effect (perhaps a vent closure far from the fire has a much greater effect than was anticipated), then the model may throttle back the fire (assuming it is a constrained fire). It is likely that the predicted soot production will then be too low (because CFAST will not increase soot production to account for the reduced oxygen) and, since temperatures are strongly affected by soot concentration, the model's temperature predictions may be grossly in error. The direct effect of the reduced heat release rate will be to lower temperatures in the vicinity of the fire, but the change in soot alters transport properties so that, further from the fire, temperatures could increase, decrease or remain the same.

The next two keywords relevant to our fire specification are FHIGH and FAREA. FHIGH is the height of the base of the flame above the position specified by FPOS. FPOS is a constant but FHIGH is treated as an event, so this keyword provides a mechanism for varying the elevation of the fire with time. For example, it could be used to simulate a debris pile in which the base of the fire decreases as the pile burns down. Since our simulations used pool fires in which the depth of the pan was negligible relative to the height of the compartment, this keyword was not needed.

FAREA specifies the horizontal area of the base of the flame. It was provided so that sophisticated plume models, in which entrainment is a function of fire area, could be incorporated into CFAST. At present, it is not used.

Finally, CJET allows the user to select either the "standard" or the "ceiling jet" model of conductive heat transfer to the ceiling. During the initial stages of a fire, the fire plume rises rapidly and may "splash" against the ceiling, spreading radially from a point above the fire. This so-called ceiling jet can heat the ceiling more efficiently than the relatively quiescent gas layer that is more typical of later times. This effect can be important during the early stages of a fire, but normally becomes insignificant as the ceiling temperature approaches that of the gas and as the upper layer becomes thick enough to act as a buffer against the rising fire plume.

The value of the CJET parameter must be either "OFF" (ceiling jet convection algorithm disabled) or "CEILING" (jet convection enabled for the ceiling). In some earlier versions of CFAST, the value "WALL" was legal and activated the jet algorithm for convection to walls. However, it was found that "WALL" produced erroneous results and, consequently, it is no longer available in CFAST 3.1.4.

2.2 Limitations Imposed by the CFAST Input Parameters

As may be seen from the above discussion, the limitations of the CFAST "vocabulary" impose certain restrictions on the nature of the problems that can be simulated. In particular, during this work we have noted the following:

a. only one internal ambient state is permitted;

b. the ceiling, floor and walls are each limited to a single set of thermophysical properties;

c. compartments can have only a single wall, which wraps around all four sides;

d. vertical vents are restricted to circular or square vents;

e. user-specified fire histories are required;

f. CFAST does not account for the variability of fire chemistry with pyrolysis and combustion conditions.

In the sections below, we discuss the impact of some of these restrictions on our ability to model the SHADWELL/688 test area and, where appropriate, the approximations and work-arounds which were developed in the process are presented.

3.0 MODELING OF THE LAUNDRY ROOM

In general, it is not good practice to "tweak" the adjustable parameters of a model in order to get acceptable agreement with experimental results. Clearly, given enough free parameters, any model can be made to fit any arbitrary data with this process. In this work, our approach has been to set as many of the inputs as possible to "real" values, *i.e.*, values which are known or believed, with some justification, to apply to the situation which we are attempting to simulate. In the case of those inputs for which we had no specific *a priori* values, we have varied the values over reasonable ranges in order to find out whether the model predictions are sensitive to these inputs. The exceptions to that rule, involving the choice of fuel mass loss rate and carbon monoxide production factor, are discussed in detail in the appropriate sections.

Details of the Submarine Ventilation Doctrine test program are given in reference [5] and will not be repeated here. However, to summarize, there were 108 fires in Series 4, of which 96 were actual tests (the rest were instrument calibration runs or demonstrations). The vast majority (78) of those tests involved fires in the laundry room and all but five of them used diesel fuel pan fires. The overall test configuration was modified several times during the series in order to create a more faithful representation of the actual submarine layout. Of the 108 tests, 65 were conducted using the final configuration.

The modifications to the basic structure (see Figure 1) included: 1) addition of partitions in the Control and Laundry Rooms to create the Navigation Equipment Room and the Laundry Passageway; 2) installation of a vertical trunk to simulate a submarine escape trunk; 3) cutting openings in the Control Room, Wardroom, Combat Systems and Crew Living decks to replicate submarine frame bays[5] and 4) installation of frame bay ducts to simulate the way in which wall panels direct smoke around the Wardroom and Crew Living spaces in an actual submarine.

Parameters which were varied during those tests included (1) open versus closed frame bays; (2) open versus closed internal doors and hatches; (3) the state of the three external hatches; and (4) fire size.

Of the many possibilities available, test 4-10 was selected to be modeled, primarily because it was the one test in which the ventilation ducts were physically blocked. This meant that it was not necessary to attempt to model the complex ventilation system and greatly simplified the problem. The specifications of test 4-10 are given in Table 2.

Table 2A provides the key for the symbols used in the remaining parts of the table. The basic test and fire description is given in Table 2B, the hatch and door configurations in Tables 2C and 2D and information regarding modifications to the test area and the specific ventilation conditions for the test is in Table 2E.

---

[5] For acoustic isolation, the decks in actual submarines do not make contact with the hull, leaving a gap between the deck edge and the hull which permits smoke and flames to spread from deck to deck. These frame bays were simulated with slots that connected between decks one and two and between decks two and three in some compartments.

Category	Code	Explanation
General		
	ND	No Data
	CD	Conflicting Data
	SD	Suspect Data
	NA	Not Applicable
	CR/WR	Connection between Control Room and Wardroom
	CS/CL	Connection between Combat Systems and Crew Living
	LP	Low Pressure
Compartments		
	LR	Laundry Room
	WR	Wardroom
	TR	Torpedo Room
	FE	Forward Escape Trunk
	CM	Crew Messroom
	CR	Control Room
	CS	Combat Systems
	FR	Fan Room
	AMR	Auxiliary Machinery Room
Test Type		
	P	Preliminary (instrument calibration and setup)
	T	Test
	D	Demonstration
Fire Type		
	Pan	Class B (diesel) pan fire
	Crib	Class A (wood) crib fire
Fire Location		
		See Compartment codes
Fuel		
	PB	Particle Board
Fire Size		
	S	Small crib
	M	Medium crib
	L	Large crib
Hatches & Doors		
	O	Open
	C	Closed
	W	Closed with watertight door
	J	Closed with joiner door
	V	Variable (state changed during test)
	SB	Closed with smoke blanket (hatches only)

Table 2A. Key for Interpreting Test Description Table

ND (No Data) is used in cases where the parameter value was not recorded; CD (Conflicting Data) means that two or more parameter values were found in different sources; SD (Suspect Data) indicates that there was reason to believe that the parameter value was erroneous.

Test ID			Fire Description					
Num.	Type	Date	Type	Loc.	Fuel	Diam. (m)	Mass Loss Rate (kg/s)	Heat Release Rate (kW)
4-10	T	01/29/96	Pan	LR	Diesel	1.05	0.0327	1310

Table 2B. Test Identification and Fire Description

Number 4-10 was a diesel fuel pan fire located in the Laundry Room. The target mass loss rate was somewhat greater than the actual value calculated from experimental data.

Hatches								
Sail		Exterior		Interior					Bilges
H01	H1	H2	H3	H4	H5	H6	H7	H8	H9-14
C	C	C	C	O	O	C	O	O	C

Table 2C. Hatch Configuration

Hatches H01 and H1 were located at the top and bottom, respectively, of the sail; H3 is the weapons loading hatch forward of the sail and H3 is the escape trunk hatch. Hatches H4 through H8 are located in the Control Room, Combat Systems, Messroom, Wardroom and Crew Living, respectively. The bilge spaces, located below AMR, the Laundry Room/Laundry Passageway and the Torpedo Room, were never used in these tests and those hatches were always closed.

Interior Doors										
D1	D1'	D2	D3	D4	D5	D6	D7	D7'	D8	D9
O	O	O	O	O	O	O	O	O	O	O

Table 2D. Interior Door Configuration

Doors are listed in order, from aft to forward and from the upper level to the lower level, with D1 at the forward end of the Fan Room and D9 at the forward end of the Torpedo Room. Note that D3 is the very small opening from the Messroom into the escape trunk.

Configuration Modifications						Ventilation							
Partition		Trunk Ext	Frame Bays			Initial Conditions		SB	IS	Diesel	LP	Pressure	
CR	LR		CR/WR	CS/CL	Ducts	Mode	Secure					CR	CS
Yes	Yes	NA	C	C	No	All off	NA	No	Off	Off	Off	No	No

Table 2E. Configuration Modifications and Ventilation

The various configuration modifications are discussed in the text. Ventilation conditions that varied from test to test included the initial state of the ventilation system and the time (after ignition) at which ventilation was secured. In some tests, internal ventilation was controlled by the use of smoke blankets, the induction system, the diesel exhaust and low-pressure blowers. In two tests, auxiliary fans were used to pressurize Combat Systems and/or the Control Room to prevent smoke infiltration into these critical spaces.

3.1 Defining the Laundry Room

In this section, we discuss the CFAST inputs that were used to model a laundry room fire, the tradeoffs that had to be made and the rationales for our choices. The dimensions of the compartment are illustrated in Figure 3.

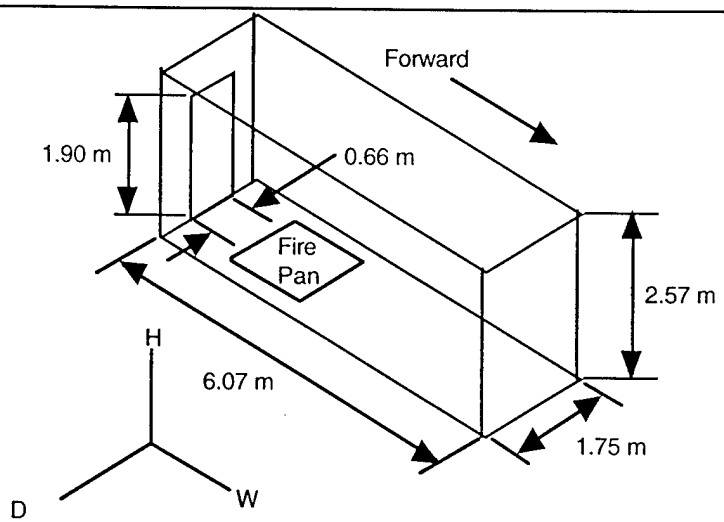

Figure 3. Laundry Room Dimensions

Configuration of the laundry room, with the fire pan centered at 0.91 (D) x 1.83 (W) x 0.19 (H). The origin of the coordinate system is the lower, left, rear corner of the compartment.

3.1.1 Simulation control

For our purposes, the only important control parameters are the simulation time and the event schedule. The actual test lasted approximately 22 minutes, but the fire began to die somewhat before that so the simulation time was set to 1250 seconds.

There was one hatch closure during the test (about six minutes after ignition), but that was in the sail, located far from the laundry room. In principle, any such closure could change the airflow

and indirectly affect the fire. However, there is no way to model this effect without including at least six additional compartments (those that were between the laundry room and the sail) and, as will be seen later, modeling most of those compartments involves making significant approximations. It was believed that, for a simple model of the fire compartment alone, ignoring the effects of the sail hatch closure would be less serious than trying to include a large number of other approximations.

The only time-related factor that directly affected the laundry room was the slow change in mass loss rate during the test. As is discussed below, this change was nearly linear, so it was sufficient to specify mass loss rates only for the start and end of the test. Accordingly, FTIME defines a single event time at 1250 seconds (recall that there is an implicit event time at zero seconds).

3.1.2 Ambient environment

Actual pre-ignition air temperatures were determined by taking the average of all air temperature readings during the period prior to ignition. The values for the laundry room and the laundry passageway (the compartment outside the laundry room door) were 285.9 K and 286.3 K, and these values were used for the initial temperature parameters for TAMB and EAMB, respectively. The rationale for using the passageway, rather than the exterior, temperature for EAMB was that, from the perspective of the fire compartment, the passageway is the exterior. That is, air entering through the door will be at passageway temperature and conduction though

the walls will be governed by the temperature difference between the laundry and the passageway. Of course, conduction through the deck and overhead areas involves other compartments, which may be at different temperatures. Most of the test area was at about the same temperature (within several degrees), so this is not likely to introduce a significant error. In any case, the limitation of being able to specify only a single "external" temperature makes this type of approximation unavoidable.

Pressures for both TAMB and EAMB were set to 101300 Pa (one atmosphere) and the reference elevations were set to zero (sea level). As was mentioned previously, the absolute elevation is significant only when modeling high-rise buildings. For a model in which the maximum elevation differences are only on the order of ten meters, these parameters are not important.

3.1.3 Model geometry

The laundry room geometry can be described very simply, with no approximations, as a 1.75 m (D) x 6.07 m (W) x 2.57 m (H) parallelepiped. Note that we have adopted the convention that width is parallel to the axis of the ship and depth is in the athwartship direction.

The elevation of the compartment deck is set to zero, which implies that it is at the same elevation as the TAMB and EAMB reference points. The joiner door leading into the laundry passageway is defined as horizontal vent number one, connecting compartment one (the laundry room) to compartment two (the exterior of the modeling domain), with a width of 0.66 m, a soffit of 1.90 m and a sill at zero. This vent is always fully open, so the CVENT parameters are set to 1.0 for both event times.

The overhead and the deck were constructed of 0.95 cm (0.375 in) steel and the characteristics of this material are defined by the SHIP3/8 entry in the thermal properties database, Thermal.df. The bulkheads, however, were made of several steel plates, having different thicknesses, welded together. Since CFAST does not permit the use of multiple materials for any single boundary, we used the area-weighted mean of the various thicknesses, which was calculated to be 0.76 cm (0.298 in.). A fictitious material, SHIPLR, was defined as having that thickness and the other parameters characteristic of steel. Since the SHADWELL spaces used during these tests were

heavily sooted, the surface emissivity was set to one, which is a reasonable value for carbon black, rather than to a value typical of clean steel. The relevant portions of Thermal.df are given in Table 3.

Material	Conductivity (W/m/K)	Specific Heat (J/kg/K)	Density (kg/m^3)	Thickness (m)	Emissivity
SHIP3/8	48	559	7854	0.0095	1
SHIP6/8	48	559	7854	0.0190	1
SHIP7/8	48	559	7854	0.0222	1
SHIP8/8	48	559	7854	0.0254	1
SHIPLR	48	559	7854	0.0076	1

Table 3. Material Property Database Entries for Steel Plate.

The material properties database (Thermal.df) used for these simulations contains several entries for the various thicknesses of steel plate used in the SHADWELL test area.

3.1.4 Fire description

The fire pan was 1.05 meters in diameter and was located in compartment one, centered at 0.91 m (D) x 1.83 m (W) relative to the lower, left, rear corner of the compartment. The load cell, used for mass loss measurements, elevated the pan 0.19 m above the deck. A constrained (type two) fire was used so that the effects of oxygen depletion would be included in the calculations.

Because the goal of this work was to determine how well CFAST simulated a specific test fire, it was very important that the fire description accurately represent the actual fire. Therefore, the mass loss rate (FMASS) inputs were based on the data from the test, as illustrated in Figure 4. To accomplish this, a three-step process was used. First, the original fuel mass data were smoothed with a five-point sliding average and plotted. Second, linear and exponential curves were fitted to these data. It was found that the exponential fit was slightly better (R^2 of 0.955 versus 0.950) than the linear so the exponential fit parameters were used for the remainder of the calculations. In the third step, these curve-fit parameters were used to calculate mass loss rate as a function of time. This rate curve was very nearly linear (R^2 greater than 0.9998 for a linear fit) and, since

CFAST uses linear interpolation between event times, the fire was specified by the mass loss rates calculated for the two event times defined by FTIME (0.0253 and 0.0229 kg/s for zero and 1250 seconds, respectively).

The exact chemistry of the fuel used for this test was not available. This is not unusual — the properties of most real fuels (as opposed to those of chemically pure surrogates, such as hexane) have high batch-to-batch variability and few batches are characterized in any significant way. However, there are a number of standards for various fuel types and we may use those standards to estimate properties for a given type.

In this case, the fuel was a marine diesel, typical characteristics for which are given in Table 4. The molecular weight and heat of combustion were taken from Table 5.2 of reference [8]. The vapor ignition temperature was based on the minimum flash point for number two diesel fuel, which is specified as 52 °C [9]. Since all refiners provide a safety margin above this minimum requirement, we assumed that the actual ignition temperature would be 10 percent higher, or 57 °C (330 K).

The lower oxygen limit and radiative fraction inputs were set to CFAST's defaults because those were believed to be reasonable values and no better information was available. In any case, the actual values of these parameters are functions of the combustion conditions and, therefore, change in an unpredictable manner during the fire. Zone models, such as CFAST, are incapable of calculating these effects so any values of these inputs must be considered only an approximation.

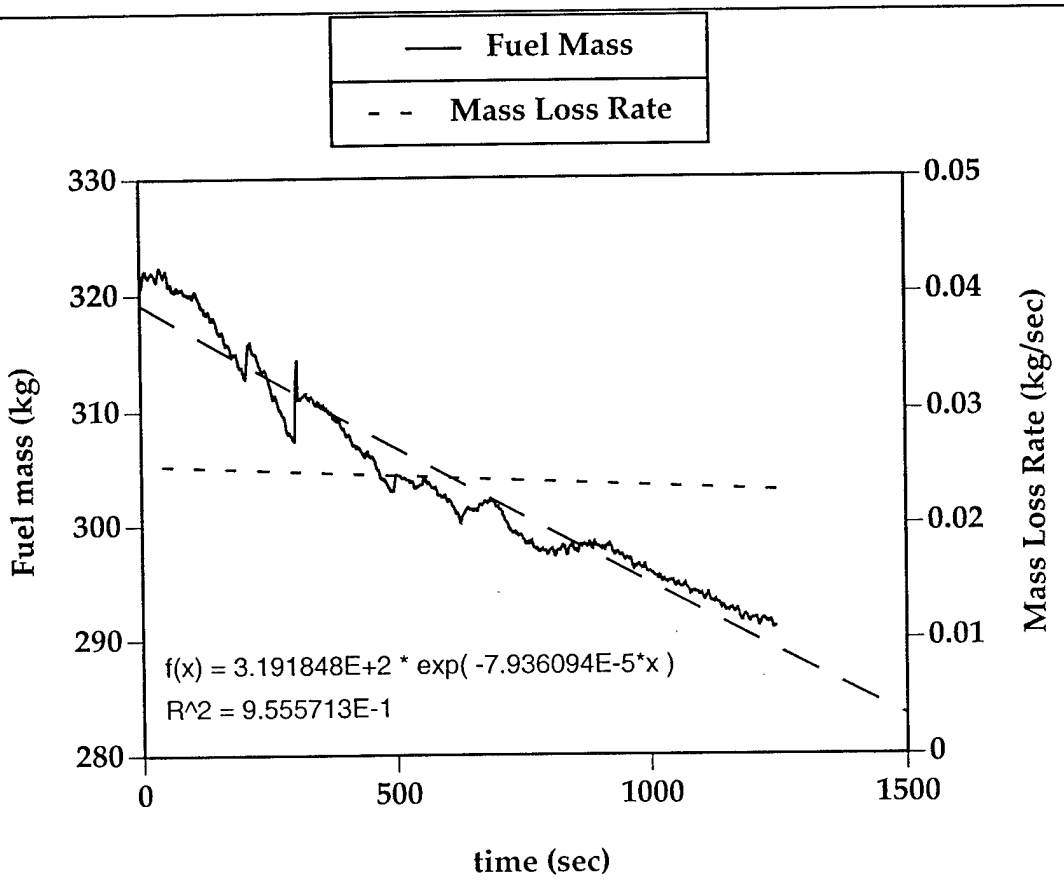

Figure 4. Fuel Mass and Mass Loss Rate

An exponential curve (long dashes) was fitted to the smoothed fuel mass data (solid curve). The curve-fit parameters shown in the figure were then used to calculate the mass loss rate, which was also plotted (short dashes).

Property	Value
Molecular weight (gm/mole)	184
Heat of Combustion (J/kg)	4.19 x 10^7
Ignition temperature (k)	330

Table 4. Typical Properties for Marine Diesel Fuel.

The initial fuel temperature was set to the laundry room ambient temperature, on the assumption that the fuel pans were approximately in thermal equilibrium with the compartment prior to ignition of the fuel. A value of 100% was used for the relative humidity.

Based on the Mil-Spec for F-76 diesel fuel [10], the minimum hydrogen content is 12.5% by weight. Assuming that the fuel was a pure hydrocarbon, the hydrogen content (per mole of fuel) is

$$184 \text{ gm fuel / mole fuel} * 0.125 = 23 \text{ gm H / mole fuel} \qquad \text{Eqn. 3}$$

and the carbon mass per mole of fuel is

$$184 \text{ gm fuel / mole fuel} - 23 \text{ gm H / mole fuel} = 161 \text{ gm C / mole fuel} \qquad \text{Eqn. 4}$$

from which we find the fuel's hydrogen to carbon mass ratio to be

$$(23 \text{ gm H / mole fuel}) / (161 \text{ gm C / mole fuel}) = 0.143 \qquad \text{Eqn. 5}$$

As an aside, the above mass values translate to molar values of

$$(23 \text{ gm H / mole fuel}) / (1 \text{ gm H / mole H}) = 23 \text{ mole H / mole fuel} \qquad \text{Eqn. 6}$$

and

$$(161 \text{ gm / mole fuel}) / (12 \text{ gm / mole H}) = 13.4 \text{ mole C / mole fuel} \qquad \text{Eqn. 7}$$

This implies that the fuel composition is approximately $C_{13}H_{23}$, which is reasonable for a diesel fuel. HCR values for several different limiting cases are discussed in a later section.

Diesel fuels have no included oxidizing agent, so the oxygen to carbon ratio is zero, and we assume that there are essentially no nitrogen- or chlorine-containing compounds in the fuel, which allows us to set the HCN and HCl ratios to zero also.

3.2 Results of Laundry Room Modeling

Since we had little guidance regarding our choices for the carbon monoxide and soot parameters, our approach was to estimate the sensitivity of the model to these inputs and, having established that, to select values that were consistent with the observed laundry room conditions. Following that, the effects of turning on the ceiling jet were evaluated and, finally, we investigated the effects of varying the HCR parameter.

The latter was done because this value can, in principle, vary over a range from less than 0.1 to greater than 0.3. Although we do have a rationale for choosing a particular value for the case at hand, we wanted to establish whether the correct choice of HCR is likely to be important for other cases.

3.2.1 Effects of CO and OD parameters on temperature

According to reference [11], for flaming fires, the maximum mass ratio of carbon monoxide to carbon dioxide is expected to be about 0.13 and CFAST's default value of the OD input, 0.05, is probably reasonable for "dirty" fuels, such as diesel, over a range of combustion conditions. However, the soot to carbon dioxide and carbon monoxide to carbon dioxide ratios are very dependent on the details of combustion which, as was noted above, CFAST can not calculate. In the absence of good values for either of these parameters, we investigated the sensitivity to values in the range zero to 0.10.

Figure 5 shows the effects on the upper layer gas temperature due to varying the OD and CO inputs. The most critical factor is the presence or absence of soot. Most of the upper layer energy is directly injected by the mass transport via the fire plume. If there is any soot (OD is non-zero), then the temperature is much lower because the sooty gas has a much higher emissivity and, therefore, cools more efficiently than does a non-sooty gas. Given the presence of soot, there is relatively little dependence on the exact soot concentration.

Higher values of the CO parameter result in essentially no change in the temperature. We expect that a higher CO parameter would reduce the soot concentration, because carbon that goes to produce CO is unavailable for production of soot, and that this would cause an increase in temperature. However, since CO is a minor constituent in the gas layer, even a large percentage increase in its concentration involves only a small decrease in the availability of carbon and this effect is negligible in most cases.

In the lower gas layer, shown in Figure 6, the trend is for increasing OD to cause an increase in temperature, which is the opposite of the trend noted above. This is because, for the lower layer, radiation is a heating, rather than a cooling, mechanism. Thus, higher soot concentrations increase the efficiency of heat absorption, leading to higher temperatures.

In this case, we do not see the overwhelming importance of the presence of soot. In fact, the temperatures in the no-soot case are virtually identical to those in the next lowest case (OD = 0.02). The effects of the CO parameter are consistent with the expectations discussed for the upper layer — increasing the amount of CO decreases the amount of soot and decreases the temperature. As before, this is a second order effect so the resulting temperature changes are relatively small. Wall, ceiling and floor temperatures (Figures 7 - 10) follow the general trend seen for the lower gas layer, except that all of the non-zero soot cases tend to cluster together. This similarity to the lower gas layer is due to the fact that, in all of these cases, the primary effect of radiation is heating.

One anomaly that should be noted is that the floor temperatures are predicted to be higher than those for the ceiling. This effect is especially apparent for the no-soot case, for which the floor temperatures are significantly higher than for the no-soot cases. Physically, the prediction that the floor is hotter than the ceiling makes little sense. Consideration of the heat transfer mechanisms involved leads to the expectation that the ceiling should always be hotter. Both surfaces are heated by convection from the adjacent gas layer and by radiation from the surroundings. Since the upper layer is at a much higher temperature than the lower, convection should make a larger contribution to heating the ceiling than the floor. In addition, convective heat transfer from a gas to a horizontal plate is more efficient when the gas is below the plate than when it is above. Thus, for the ceiling, there is more energy available in the adjacent gas layer and a greater percentage of it should be transferred to the surface by convection. The upper layer is the primary source of radiative heating for all surfaces, due to its significantly higher temperature and to the T^4 dependence on emission. Also the upper layer typically occupies most of the volume in the fire compartment and, therefore, the radiative heating component should be similar for the floor and ceiling.

Of course, the above implicitly assumes that the floor and ceiling material properties are the same. Clearly, if there are significant differences in the emissivities, heat capacities, conductances or other thermal properties, then expectations based on heat transfer arguments may be erroneous. However, in this case, the ceiling and floor reference the same entry in the thermophysical database, so this anomaly can not be explained so easily. At present, the reason for the discrepancy between expected and observed behavior is unknown but is believed to be due to an error in CFAST. This anomaly, which is considered in more detail in the discussion

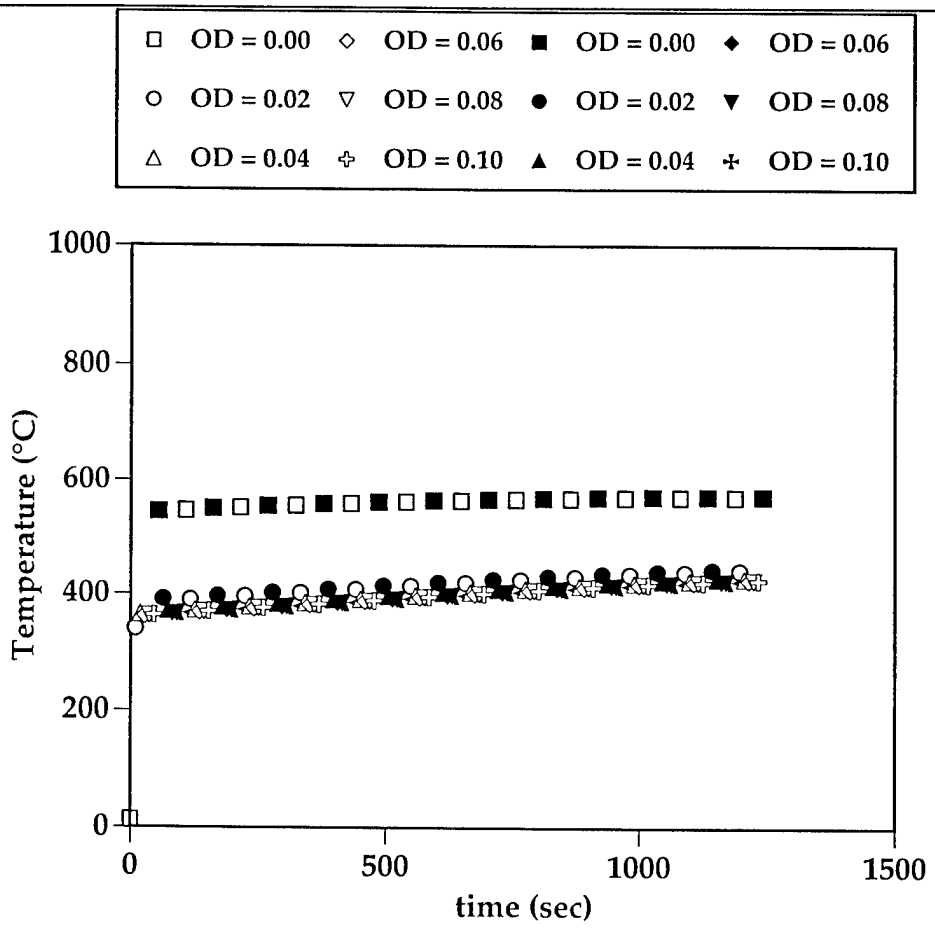

Figure 5. Upper Layer Gas Temperature as a Function of OD and CO Parameters

Upper layer gas temperature shows almost no dependence on the carbon monoxide concentration, which is determined by the value of the CO parameter. There is a strong dependence on the amount of soot, controlled by the OD parameter. (Open symbols: CO = 0.00; solid symbols: CO = 0.10).

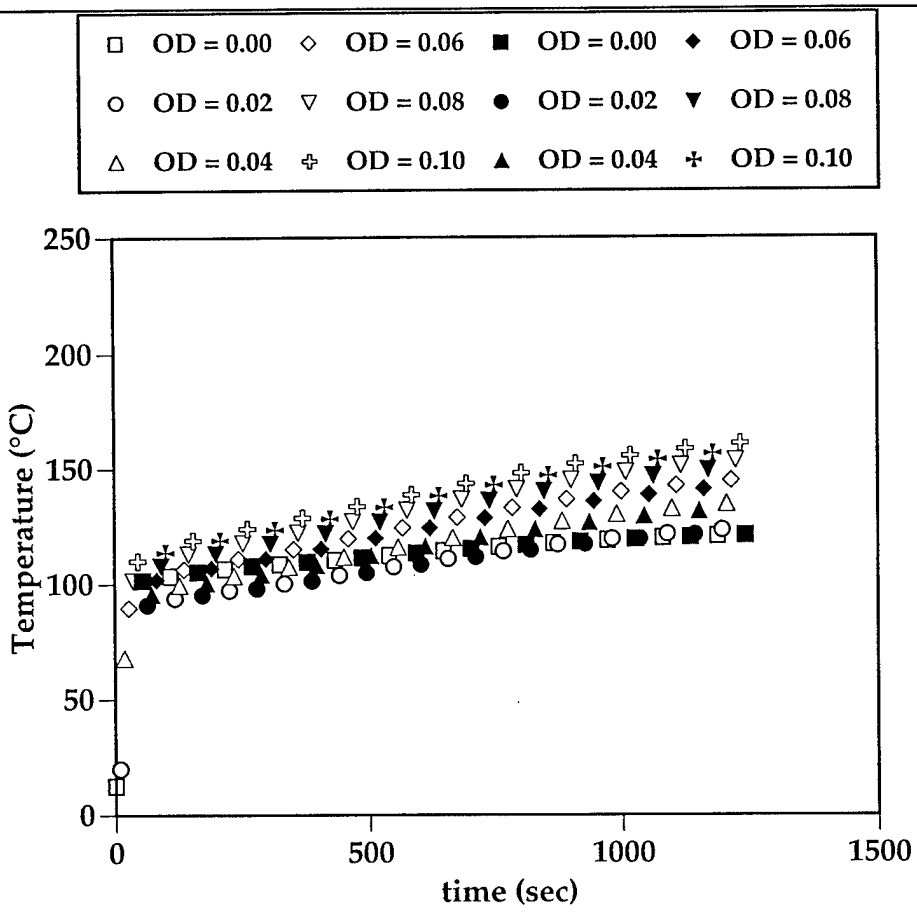

Figure 6. Lower Layer Gas Temperature as a Function of OD and CO Parameters

Lower layer gas temperature is dependent on both the CO and the OD parameters, but the effects of OD predominate. (Open symbols: CO = 0.00; solid symbols: CO = 0.10).

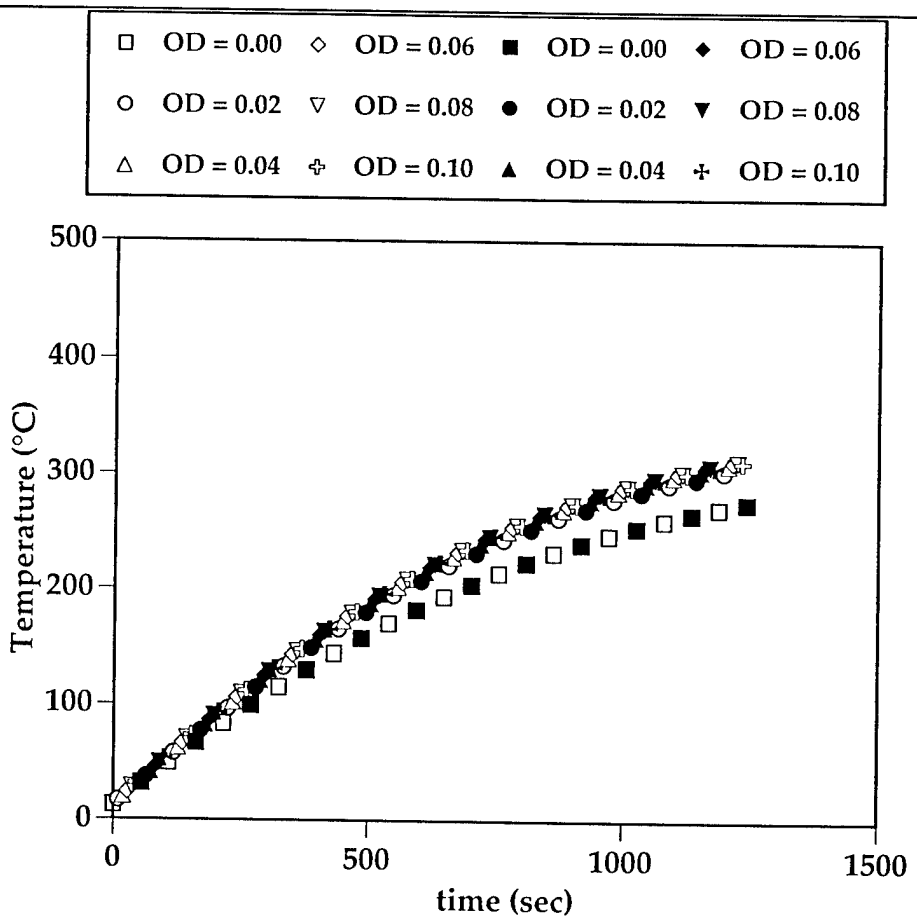

Figure 7. Upper Wall Temperature as a Function of OD and CO Parameters

Upper wall temperatures are relatively independent of CO and OD, except for the no-soot case where the low absorbance leads to a reduced temperature. (Open symbols: CO = 0.00; solid symbols: CO = 0.10).

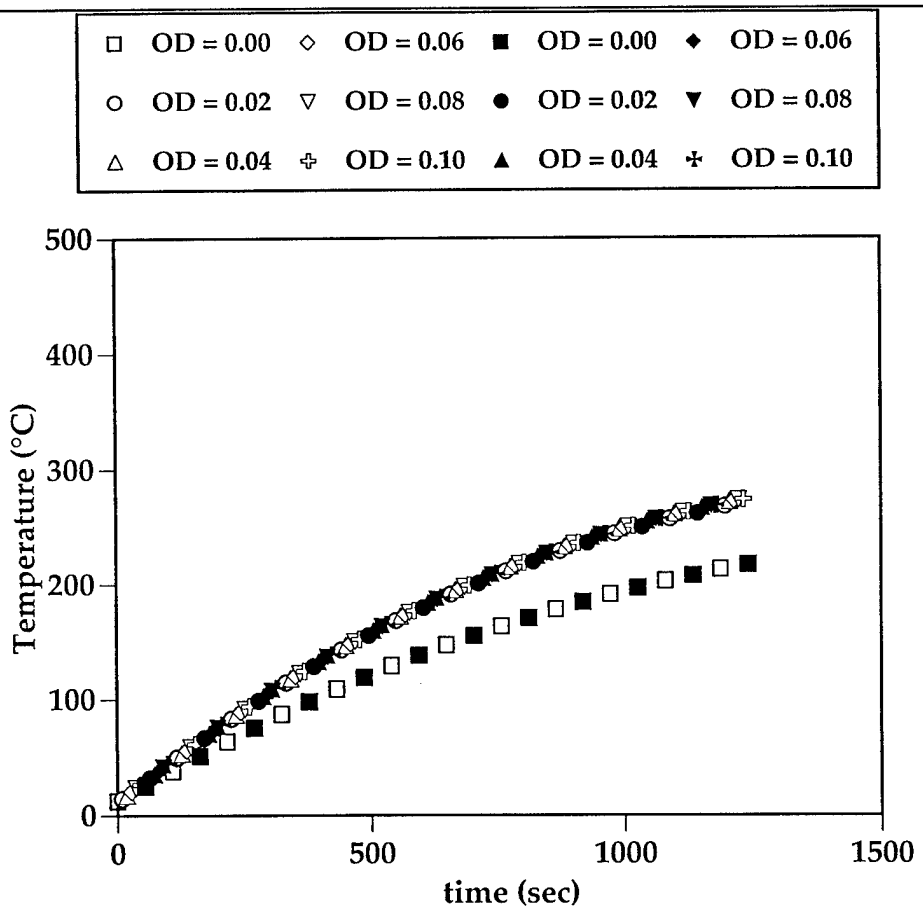

Figure 8. Lower Wall Temperature as a Function of OD and CO Parameters

Lower wall temperatures follow the same trends that were seen for the upper walls but the absolute values are lower. This is attributed to the lower temperature of the adjacent gas layer. (Open symbols: CO = 0.00; solid symbols: CO = 0.10).

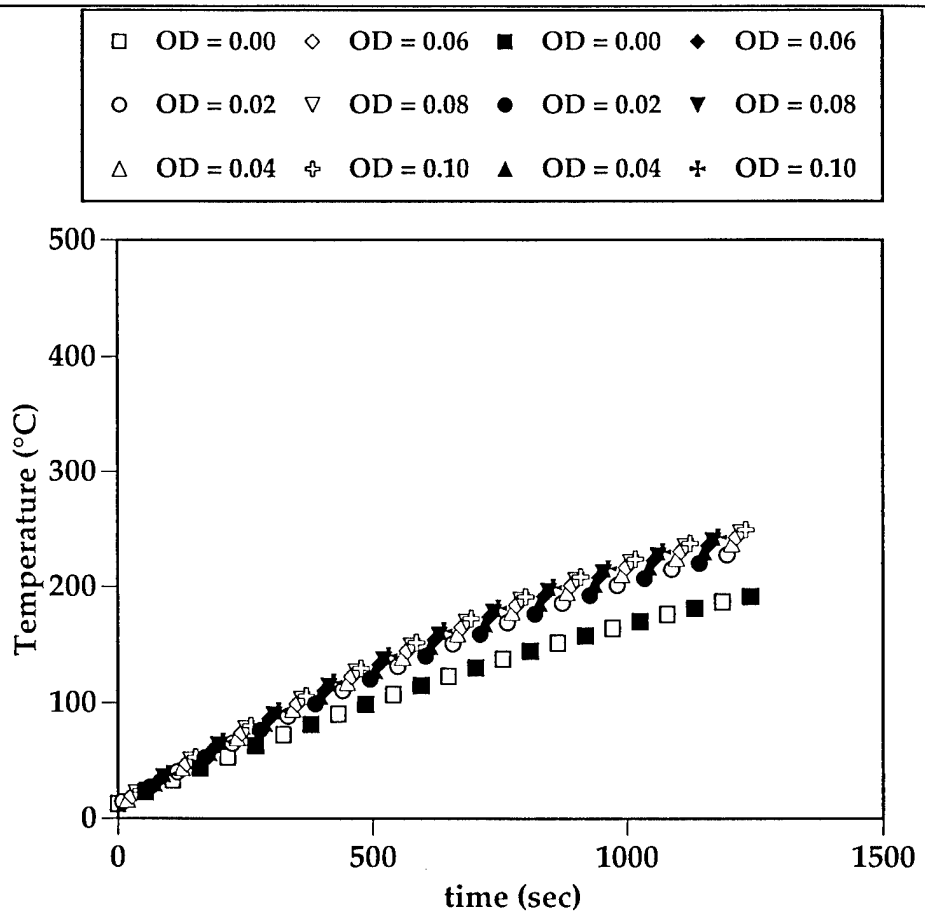

Figure 9. Ceiling Temperature as a Function of OD and CO Parameters

Ceiling temperatures also follow the pattern of the upper wall, as is expected. However, the absolute temperatures are unexpectedly low relative to the upper wall. (Open symbols: CO = 0.00; solid symbols: CO = 0.10).

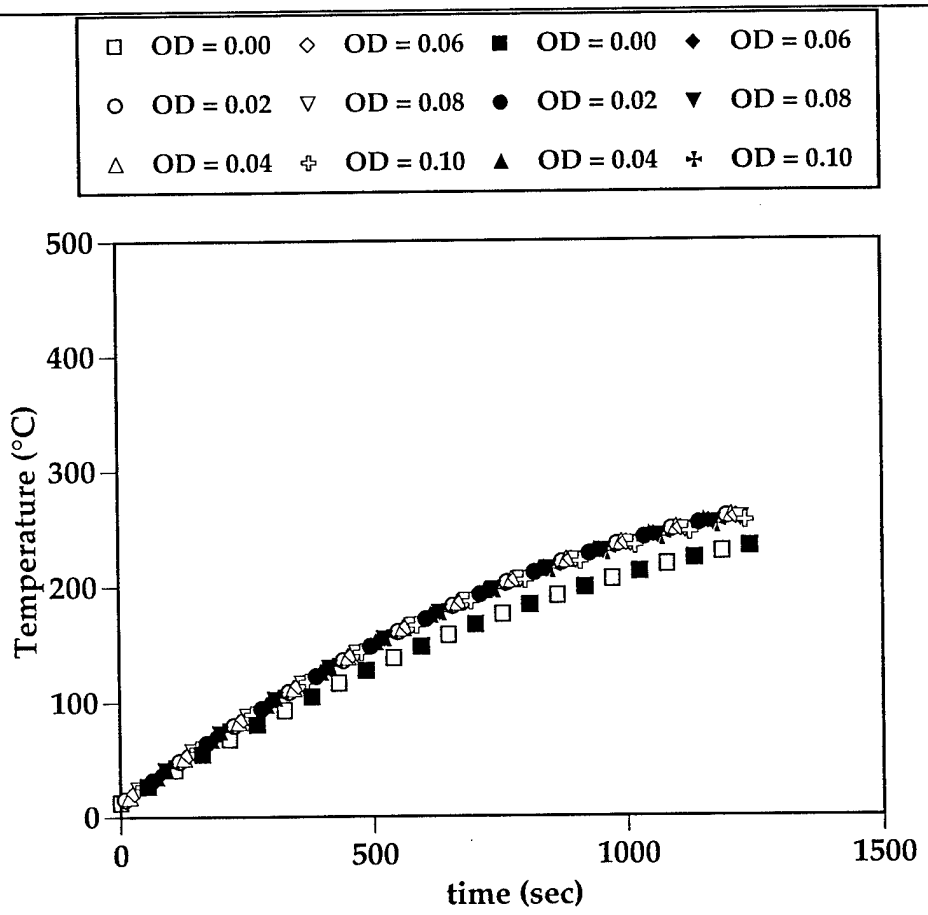

Figure 10. Floor Temperature as a Function of OD and CO Parameters

Floor temperatures, as is expected, are comparable to the lower wall temperatures. (Open symbols: CO = 0.00; solid symbols: CO = 0.10).

section below, did not appear in several previous simulations of other fire scenarios, so it is likely due to some factor specific to the Laundry Room configuration.

3.2.2 Effects of CO and OD parameters on species concentration

The values of CO and OD have essentially no effect on the upper or lower layer oxygen concentrations (Figures 11 and 12). One might expect that, as either of these parameters is increased, the fraction of carbon which is converted to carbon monoxide or soot would increase at the expense of carbon dioxide, leading to lower oxygen consumption and, therefore, to higher oxygen concentrations. However, for reasonable CO and OD values, carbon dioxide is the dominant carbon species by a large margin. In this case, even large percentage changes in the concentrations of the minor carbon species will have a relatively small effect on carbon dioxide concentration. Since, in this simulation, only a fraction of the oxygen reacts with the fuel, the net effect is that there is no significant effect on the oxygen consumption and, therefore, no appreciable effect on the residual oxygen concentration.

As you might expect, these two parameters have a larger effect on the concentration of carbon dioxide than they do on the oxygen concentration. Figure 13 shows that, for a given value of the CO input, carbon dioxide concentration decreases with increasing OD because more of the available carbon is tied up as soot. Likewise, increasing the carbon monoxide fraction in the combustion products causes a reduction in carbon dioxide. Both of these trends are repeated in the lower layer (Figure 14), except for the case of OD equal to zero. In that case, the carbon dioxide concentration is approximately the same as for OD = 0.08 - 0.10 at the beginning of the simulation and is similar to OD = 0.02 - 0.04 at the end.

Of course, setting the CO parameter to zero makes the carbon monoxide concentration identically zero, regardless of the value of the OD parameter. When CO is not forced to zero, carbon monoxide concentrations follow the same basic patterns that were seen in the case of carbon dioxide — declining as the amount of soot increases, except for the no-soot situation in the lower layer which, again, is a special case (Figures 15 and 16).

The reason that the lower layer, no-soot case differs from the trends established for the other cases is not understood. However, it may be related to the fact that the upper layer temperatures for this case are also significantly different than for the other cases. This could have indirect effects on the mixing between the upper and lower layers, leading to both different concentrations and different rates of change of the concentrations.

CFAST reports soot concentrations in units of 3500 fV, where fV is the volume fraction. In Figures 17 and 18, we have converted these values to mass concentrations (kg/m^3), using 1800 kg/m^3 as a typical density for amorphous carbon. Soot concentrations are approximately linear with the OD parameter value and show the expected reduction in soot production as the CO parameter is increased. The trends are the same for both layers but, of course, the absolute concentrations are several times greater in the upper layer. In addition to its effects on temperature, soot concentration is an important habitability parameter because of the increased atmospheric toxicity and the reduced visibility that it causes.

Note that we see increasing oxygen and decreasing carbon dioxide, carbon monoxide and soot, in both the upper and lower layers, while the fire is still burning. This would seem to indicate that, after the ignition transients, the bulk flows settle into a near steady state which supplies fresh air at an approximately constant rate. Since the combustion rate is slowly declining (see Figure 4), the net result is a slow increase in oxygen and decreases in combustion products. Mixing in the fire plume and door jet cause this effect to appear in both layers.

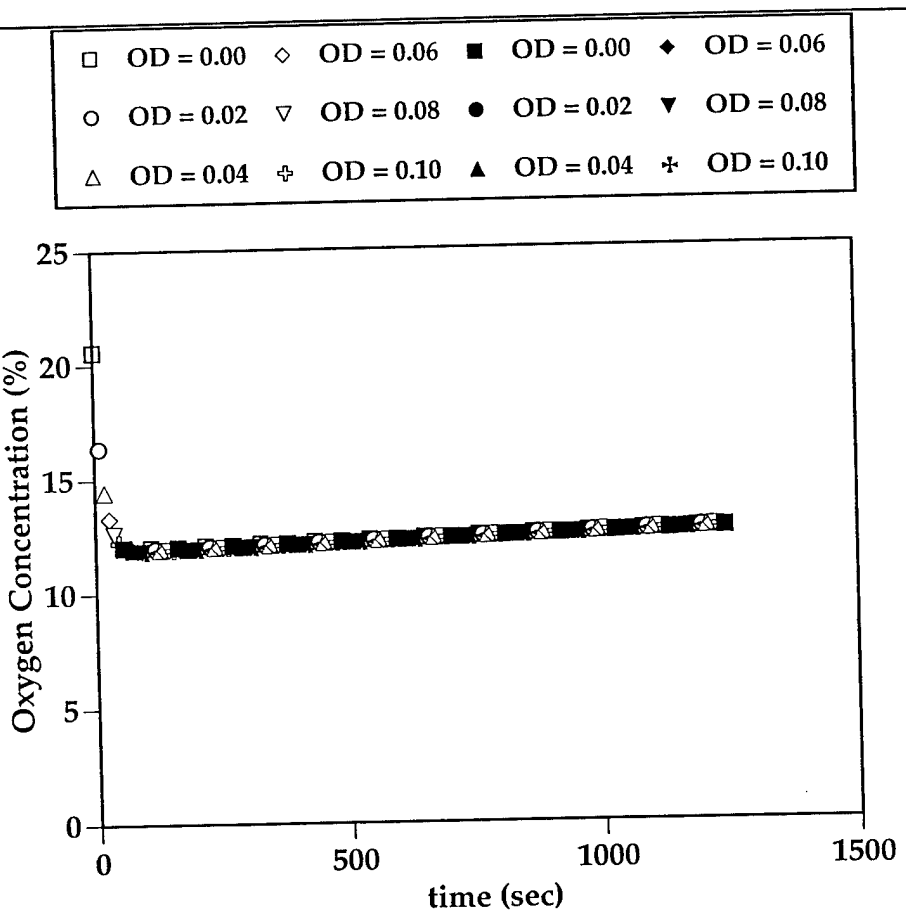

Figure 11. Upper Oxygen Concentration as a Function of OD and CO Parameters

Carbon dioxide is the predominant combustion product and is the controlling factor in oxygen concentration, therefore, neither of the OD nor the CO parameters has a significant effect. Oxygen is severely depleted in the upper layer because combustion products from the fire are directly injected by the fire plume. (Open symbols: CO = 0.00; solid symbols: CO = 0.10).

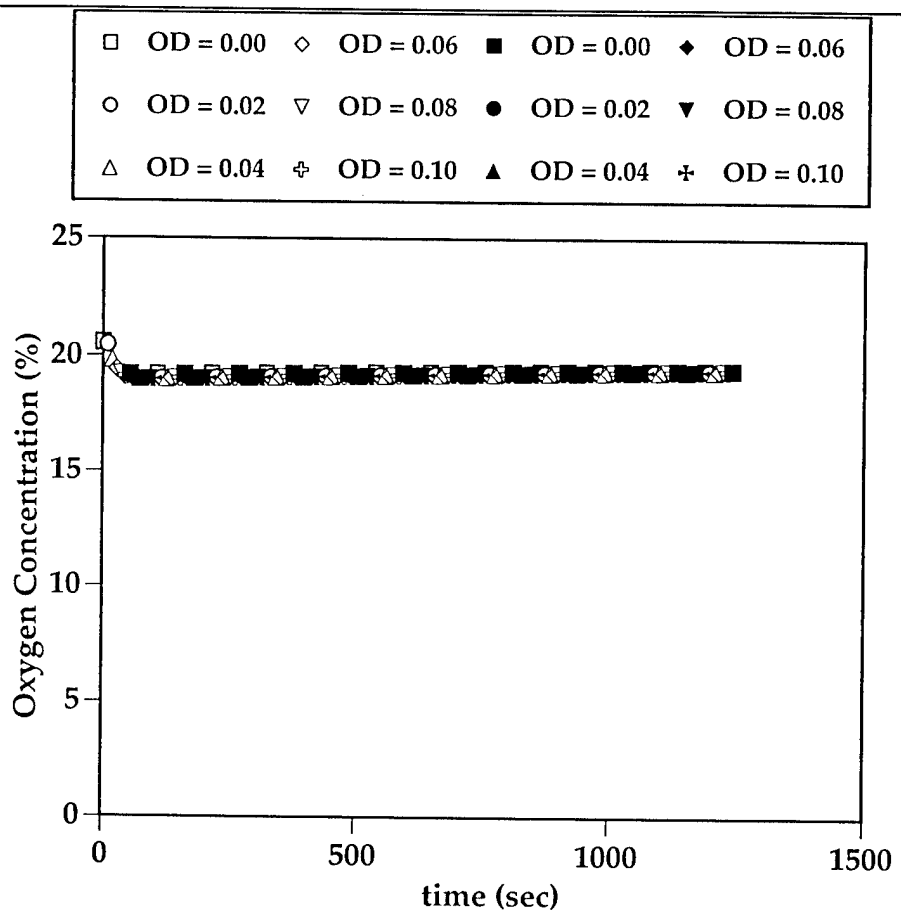

Figure 12. Lower Oxygen Concentration as a Function of OD and CO Parameters

As in the upper layer, neither parameter has a significant effect on the oxygen concentration. Since CFAST does not include direct mixing of combustion products from the upper layer into the lower layer, there is a relatively small decrease in lower layer oxygen concentration. (Open symbols: CO = 0.00; solid symbols: CO = 0.10).

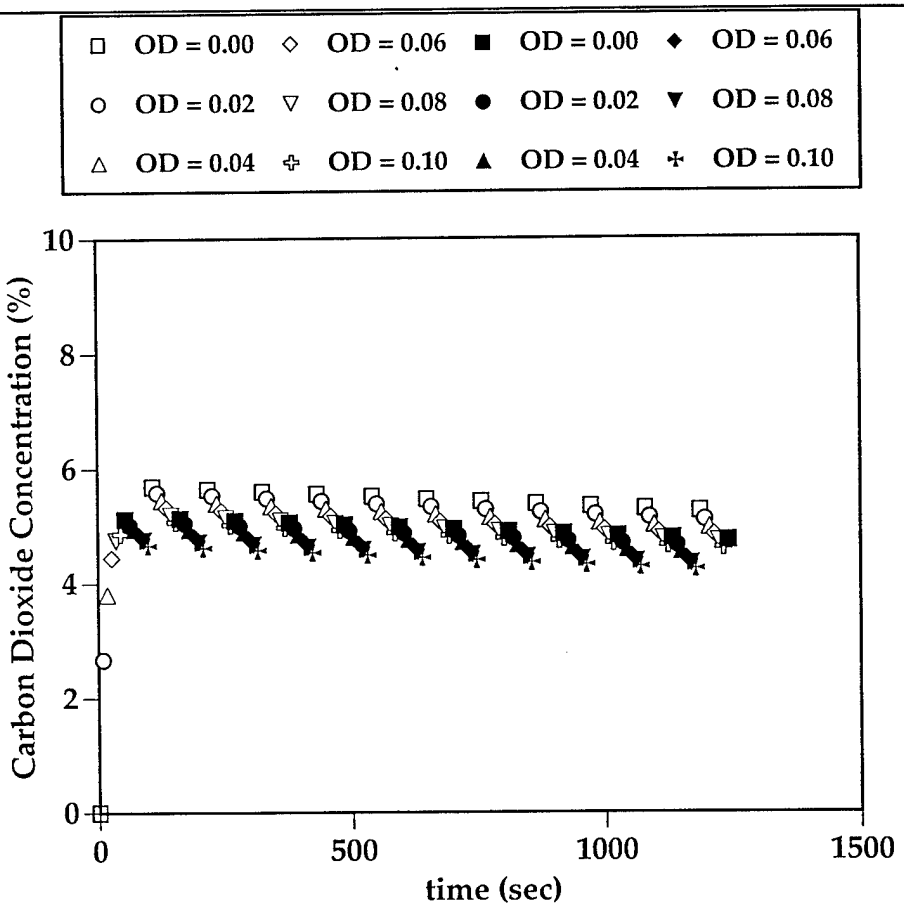

Figure 13. Upper Carbon Dioxide Concentration as a Function of OD and CO Parameters

Because carbon monoxide and soot are relatively minor constituents of the combustion products, even large percentage changes in their concentrations have small effects on the concentration of the dominant constituent, carbon dioxide. (Open symbols: CO = 0.00; solid symbols: CO = 0.10).

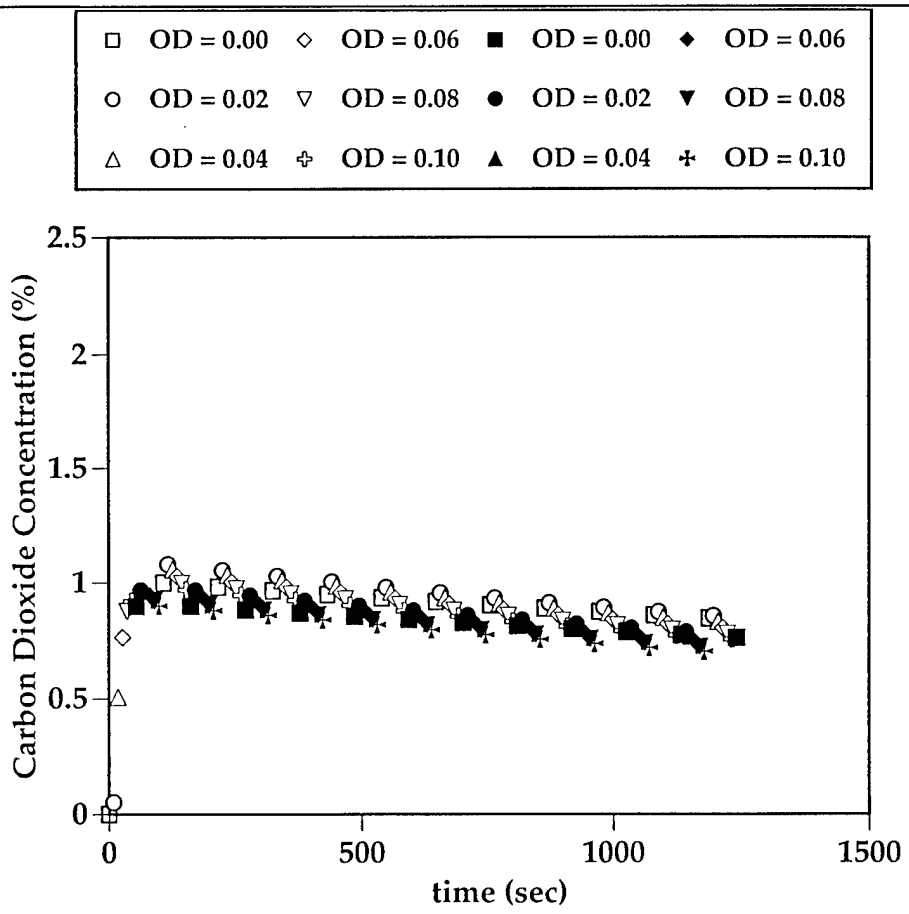

Figure 14. Lower Carbon Dioxide Concentration as a Function of OD and CO Parameters

The behavior of carbon dioxide in the lower layer is qualitatively similar to that in the upper layer, except in the absence of soot. For that case, the initial concentrations are less than expected and the rate of decrease is also lower than for the other cases. (Open symbols: CO = 0.00; solid symbols: CO = 0.10).

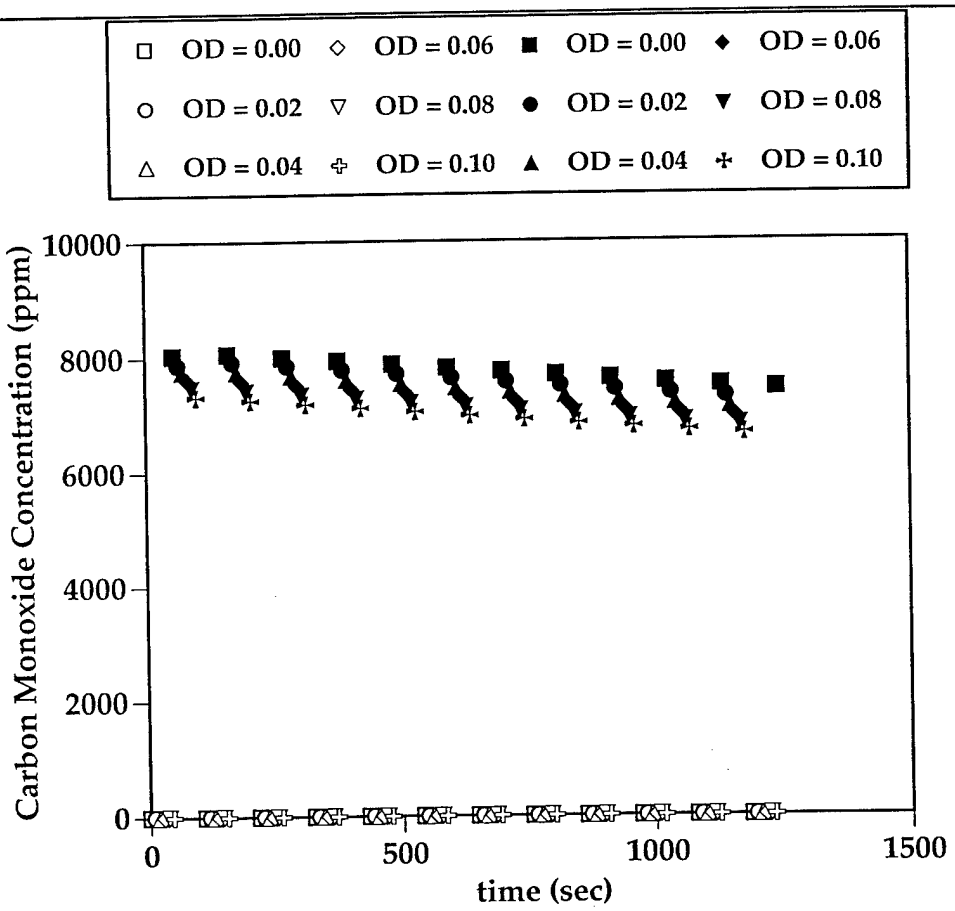

Figure 15. Upper Carbon Monoxide Concentration as a Function of OD and CO Parameters

The behavior of carbon monoxide is qualitatively similar to that of carbon dioxide, unless the CO parameter is set to zero, in which case the model completely suppresses the creation of carbon monoxide. (Open symbols: CO = 0.00; solid symbols: CO = 0.10).

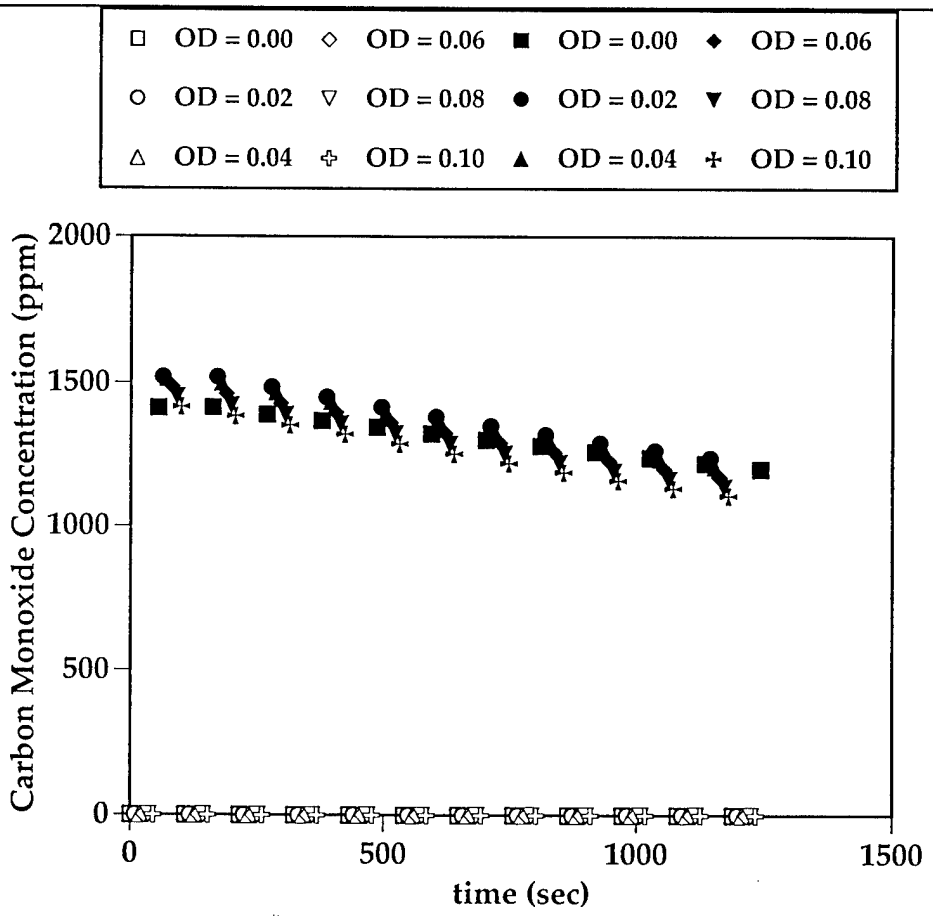

Figure 16. Lower Carbon Monoxide Concentration as a Function of OD and CO Parameters

As in the case of carbon dioxide, lower layer carbon monoxide follows the expected trend for non-zero values of the OD input. (Open symbols: CO = 0.00; solid symbols: CO = 0.10).

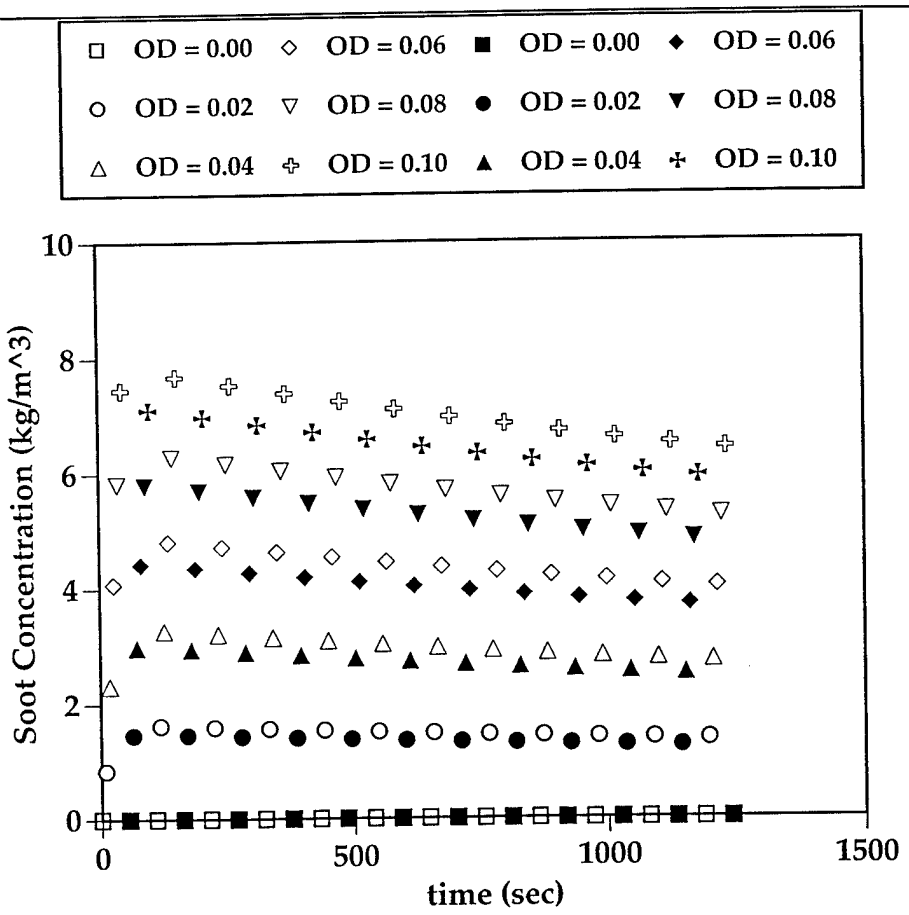

Figure 17. Upper Soot Concentration as a Function of OD and CO Parameters

Upper layer soot concentrations increase approximately linearly with OD and, as expected, decrease with increasing values of the CO parameter. (Open symbols: CO = 0.00; solid symbols: CO = 0.10).

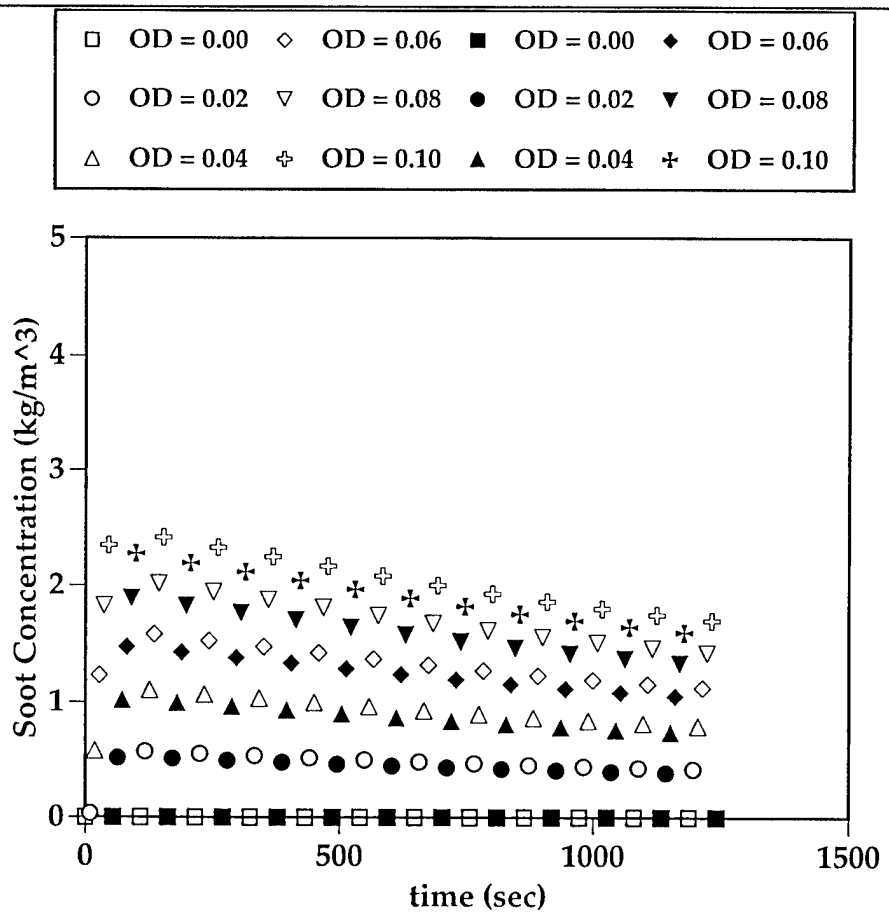

Figure 18. Lower Soot Concentration as a Function of OD and CO Parameters

Soot concentrations in the lower layer follow the same pattern as seen in the upper but the absolute concentration values are lower, in keeping with the "cleaner" nature of the lower layer. (Open symbols: CO = 0.00; solid symbols: CO = 0.10).

3.2.3 Selection of CO and OD parameters

Based on the above, it appears that the choice of the CO parameter value is not very critical, except for prediction of carbon monoxide concentration. Therefore, if the purposes of the simulation do not require accurate predictions of carbon monoxide concentration, any reasonable value is probably adequate. On the other hand, if accurate carbon monoxide predictions are required, then the choice of a CO parameter value becomes problematical.

The actual value of this parameter varies with time and is highly dependent on the details of the combustion process. As an example, the laundry room carbon monoxide to carbon dioxide mass ratio, calculated from experimental gas analysis data, is shown in Figure 19. This ratio varies in a complex manner over the duration of the test and is obviously not something that can be reliably estimated unless the user has a significant amount of *a priori* knowledge about the fire.

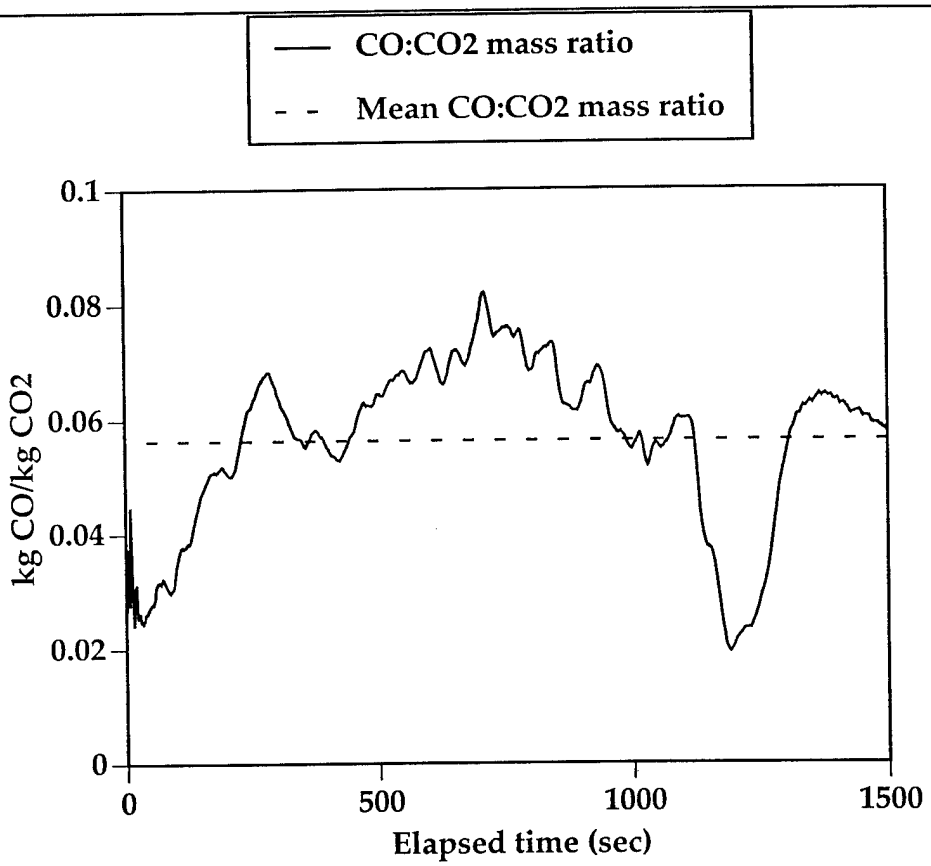

Figure 19. Experimental Carbon Monoxide to Carbon Dioxide Ratio

The actual carbon monoxide to carbon dioxide mass ratios were calculated from fire compartment gas analysis data and the mean value, 0.056, was used as the CO parameter input for subsequent CFAST simulations.

In the absence of such knowledge, it is probably best to select a nominal value, based on whatever information is available, and bracket that value with high and low extremes. In our case, we do have access to gas concentration information, so we have chosen to apply that knowledge by using the mean mass ratio for the test, 0.056, as the standard CO input value. This is similar to our previous application of experimental mass loss rate data to estimate the heat production rate of the fire.

The OD parameter plays a very important part in the prediction temperature and visibility. It contributes to toxicity predictions both directly, through the soot concentration, and indirectly, through its effects on oxygen, carbon dioxide and carbon monoxide. As a result, selecting a "good" value for this parameter is critical for the three most common applications of CFAST — prediction of fire spread, habitability and egress times. Outside of the heat release rate of the fire, the OD input is probably the single most important fire parameter because it affects so many important aspects of the model.

Like the CO input, the OD is variable and is dependent on combustion chemistry. Also like CO, selecting a "correct" value requires knowledge that in unlikely to be available to most users. Fortunately, based on the above sensitivity analysis, it appears that, for a "clean" fire (propane or methanol, for example), a value of zero is appropriate for most predictions. As we have seen, increasing the OD input usually has diminishing effects above about 0.04, therefore, for a "dirty" fire (most fires of interest to the Navy), a value in the range of 0.06 is probably reasonable.

Of course, if the actual concentration of soot is important, then the above estimate should not be applied and more detailed information will be needed. However, in most cases, it is probably sufficient simply to predict the point at which the temperature, habitability or egress time reaches a threshold value. For these purposes, the above rule of thumb is expected to be satisfactory.

In the following sections, we investigate the sensitivity of CFAST to two additional inputs, CJET and HCR. In order to reduce the complexity of this work, we have adopted standard values for all of the parameters discussed above. Because we know that diesel fuel produces a typical "dirty" fire, we use 0.06 as the nominal OD parameter, but we also bracket this with values of zero and 0.10 in order to obtain a better feel for the effects of this parameter. The CO input is set to 0.056, as was discussed above.

3.2.4 Effects of the CJET parameter

In the absence of any theoretical justification for selecting a setting for the ceiling jet parameter, we ran the model with the ceiling jet off and with it on and compared the resulting temperature predictions. Because this parameter only affects the ceiling heat transfer calculations, it was not necessary to consider the effects on species concentrations. For a similar reason, we consider only effects on the ceiling temperature.

Figure 20 clearly shows that the CJET parameter has no detectable effects on the predicted ceiling temperatures. As was mentioned previously, CJET would be expected to have a significant effect only during the period during which the upper layer is developing. Since, in most cases of Naval interest, the upper layer develops virtually instantaneously, it is not surprising that CJET effects are of such a short duration that they are not detectable. As a result of this finding, we chose to turn the CJET algorithm off for the remainder of this study.

3.2.5 Effects of the HCR parameter

As was discussed previously, water vapor, soot and carbon dioxide all contribute to radiation absorption. We have seen that the latter two species can have significant effects on temperatures, so it is reasonable to investigate the effects of changing the water vapor concentrations.

Like soot and carbon monoxide, water vapor concentration may be adjusted by the user through selection of inputs. In fact, water vapor concentration is controlled by two different inputs, the relative humidity and the HCR parameter. The former sets the initial water concentration prior to ignition while the latter affects the rate at which water vapor is produced during combustion. Unlike the OD and CO parameters, which specify combustion product concentrations as a

fraction of the concentration of another combustion product (carbon dioxide), HCR is based on the composition of the fuel.

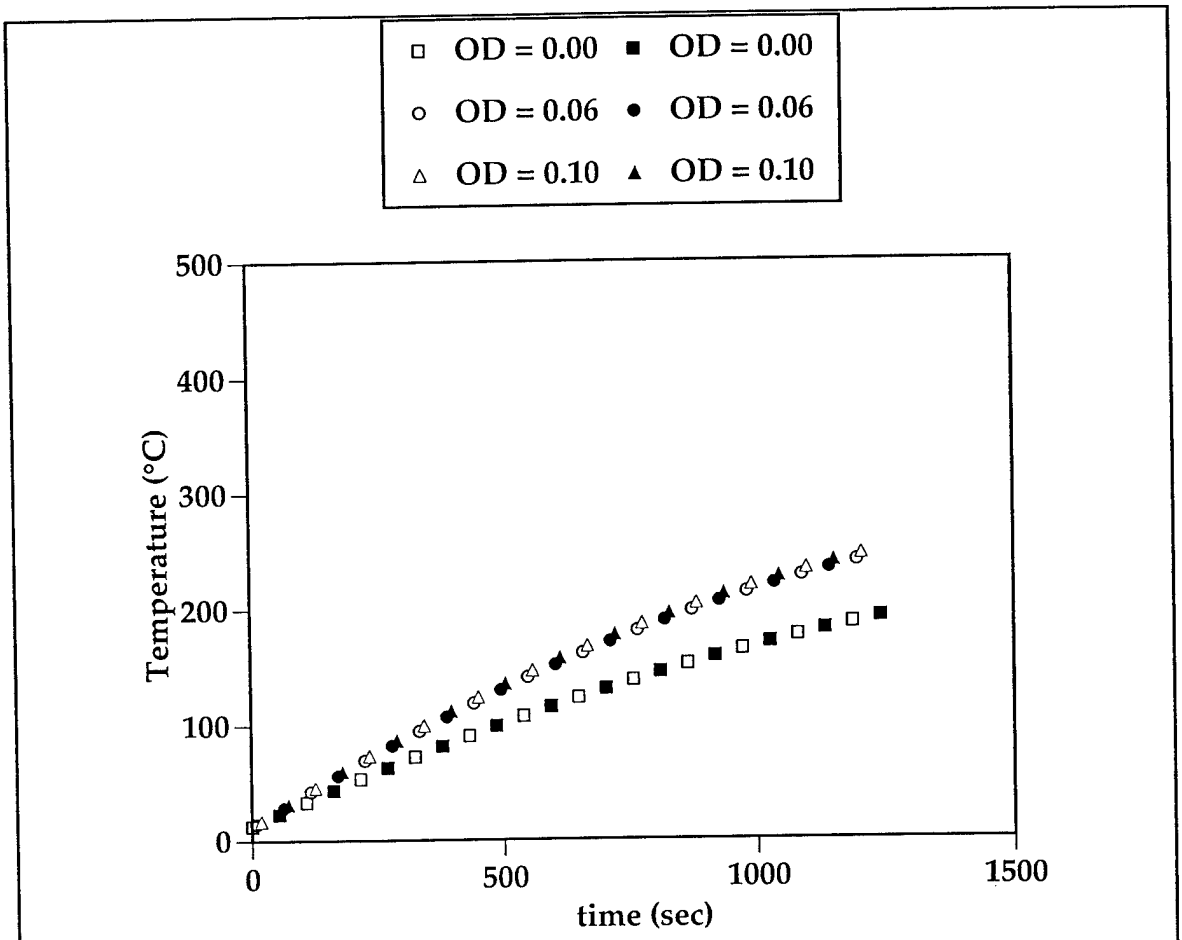

Figure 20. Ceiling Temperature as a Function of OD and CJET Parameters

Predicted ceiling temperatures are not sensitive to the CJET setting, which controls the type of algorithm used for calculation of heat transfer into the ceiling. (Open symbols: CJET = OFF; solid symbols: CJET = CEILING).

This is significant because, whereas the combustion product ratios are necessarily complex functions of the combustion process, the fuel composition is independent of those processes and, in principle, may be known in advance. Thus, although actual fuel composition may be variable, there is a physical basis for expecting HCR to lie within a specific range for a given fuel type.

For our fuel, the nominal HCR value was seen to be 0.143 (Equation 5). This value was used to obtain the model results discussed above. However, we can make some reasonable estimates of the range of possible HCR values as follows:

For hydrocarbon fuels, the minimum HCR will be found in long-chain, highly unsaturated molecules,

$$H—(C \equiv C)_n—H$$

having a generic molecular formula of $C_{2n}H_2$. The hydrogen to carbon mass ratio is then

$$HCR = 2 / (12 * 2 * n) = 0.083 / n \qquad \text{Eqn. 8}$$

which, for large n, approaches zero. As a test, we attempted to set HCR to zero but found that the model then would not run for the no-soot case. However, the model did run with non-zero OD inputs. It was determined empirically that the smallest HCR for which the model reliably executed was about 0.05, which was used as the lower limit in these calculations.

Of course, the fuel postulated above is hypothetical — such a high degree of unsaturation would be extremely unstable. The only practical fuel of this type is acetylene (n = 1) with an HCR of 0.08. Thus, the lowest usable HCR value happens to be very close to the lowest physically reasonable value.

At the other extreme, the maximum HCR corresponds to a short-chain, saturated hydrocarbon for which the limiting case is methane, CH_4, with an HCR of 0.33. Again, the model would not run to completion with this input, so a value of 0.30 was used for the upper limit calculations. We also note that the generic formula for alkanes is C_nH_{2n+2}, for which the long-chain limiting case gives an HCR value of 0.167, not far from the 0.143 used in this work.

The value of HCR was found to have no significant effect on temperature, except in the lower gas layer. Figure 21, the upper layer temperature, shows the typical case while Figure 22 illustrates the situation for the lower layer. For non-zero OD, increasing the value of HCR has the same qualitative effect as decreasing the value of OD.

Naively, we might expect that absorbance due to soot would overwhelm that due to gases and, therefore, that there would be negligible temperature difference among the non-zero soot cases. In the case of zero soot, all absorbance is due to gases and we might expect that there would be small temperature differences. However, since increasing HCR would increase water vapor and decrease carbon dioxide, it is not obvious whether the absorbance should increase, decrease or, in the event that the effects offset, stay about the same.

The upper layer results are generally in agreement with this analysis but, for the lower layer, it is clearly wrong — the temperature differences are very small for the no-soot case and much greater when there is soot. In the following section, we will revisit these questions using a less naive analysis.

3.2.6 Standard model input parameters

Based on the considerations discussed in the previous three sections, we have established a standard set of fire specification parameters for modeling of Submarine Ventilation Doctrine test 4-10, as shown in Table 5. We intend to use these values in future simulations in order to maintain a consistent fire definition. Listing 5 is an example of a standard input files as used in these simulations.

3.3 Discussion of Laundry Room Predictions

We saw that our CFAST simulation predicted floor temperatures higher than the ceiling temperatures and that this appears to be a non-physical result. We have also seen that, for hydrocarbon fuels[6], three parameters (HCR, OD and CO) control CFAST's combustion

[6] We specify hydrocarbons because the additional parameters HCl, HCN and O2 are important for fuels that contain chlorine, nitrogen or oxidizer.

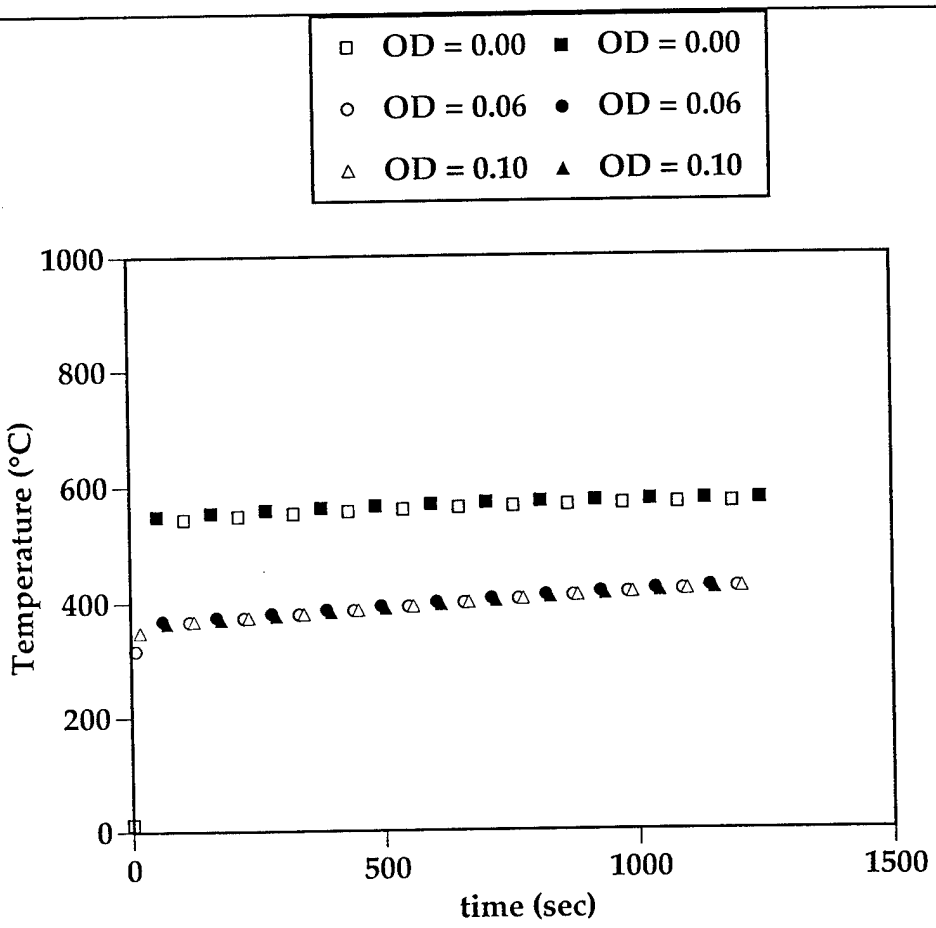

Figure 21. Upper Layer Gas Temperature as a Function of OD and HCR Parameters

The value of HCR has virtually no effect on the upper layer gas temperature or on the wall, floor or ceiling temperatures (not shown). (Open symbols: HCR = 0.05; solid symbols: HCR = 0.30).

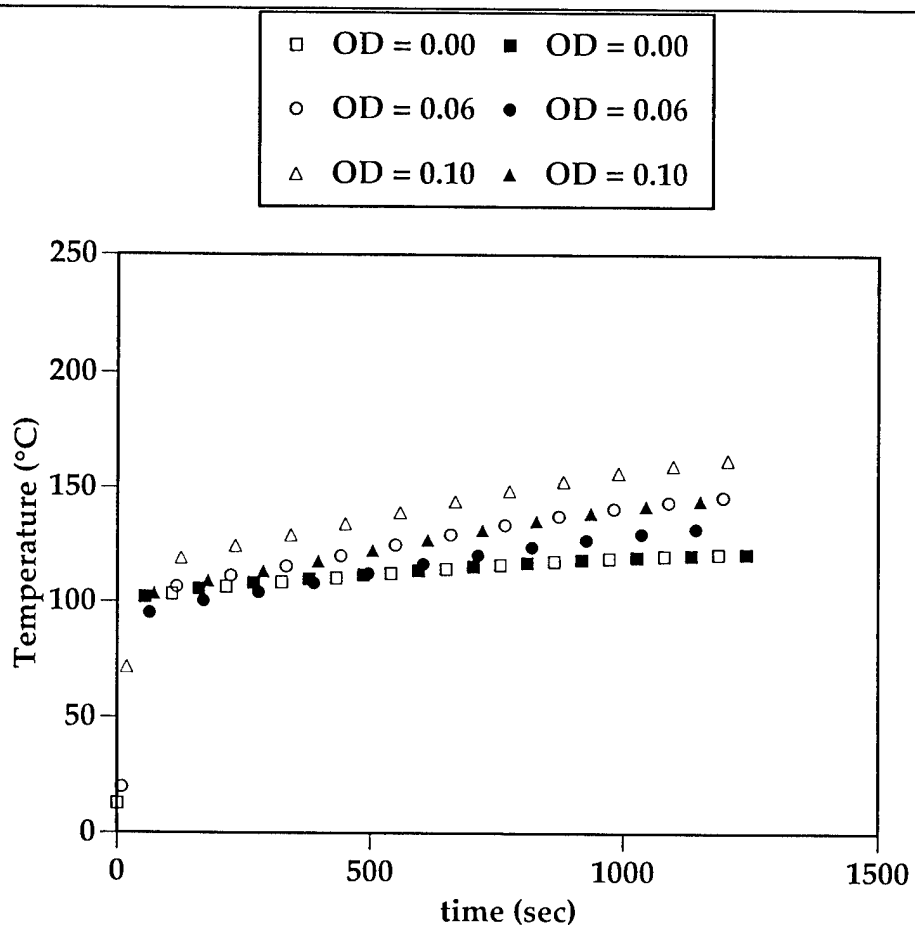

Figure 22. Lower Layer Gas Temperature as a Function of OD and HCR Parameters

The lower layer gas is the exception to the rule. In this case, increasing HCR reduces the temperature, suggesting that the gas absorption has been reduced. (Open symbols: HCR = 0.05; solid symbols: HCR = 0.30).

chemistry model and that there are interactions among these parameters which sometimes make it difficult to predict the effects that should be expected if any one of them is changed.

In this section, we will investigate the floor/ceiling temperature anomaly and try to determine its cause. We will then consider the interactions among the three main combustion chemistry parameters and develop a simplified set of equations, which can be used to estimate their interactions.

3.3 Discussion of Laundry Room Predictions

We saw that our CFAST simulation predicted floor temperatures higher than the ceiling temperatures and that this appears to be a non-physical result. We have also seen that, for hydrocarbon fuels[7], three parameters (HCR, OD and CO) control CFAST's combustion chemistry model and that there are interactions among these parameters which sometimes make it difficult to predict the effects that should be expected if any one of them is changed.

In this section, we will investigate the floor/ceiling temperature anomaly and try to determine its cause. We will then consider the interactions among the three main combustion chemistry parameters and develop a simplified set of equations, which can be used to estimate their interactions.

Parameter	Standard Value	Comments
CO	0.056	Derived from experimental measurements.
OD	0.06	Appropriate for sooty fires
CJET	OFF	Expected to affect only the ceiling temperature during the first few seconds.
HCR	0.143	Estimated from diesel fuel properties.

Table 5. Standard Fire Specification Parameters for Submarine Ventilation Doctrine Test 4-10

These values were adopted as "standard values" for the fire specification for Submarine Ventilation Doctrine test 4--10, based on the results of a sensitivity analysis which used a wide range of inputs.

3.3.1 The floor/ceiling temperature inversion anomaly

We had never seen this anomalous behavior in previous work and it was unclear whether it was due to the specifics of this simulation or to something intrinsic to the CFAST model. In an effort to identify the source of the error, we reran a test case using CFAST version 2.1 and compared the results with the predictions from version 3.1.4.

A value of 0.06 was chosen for the CO parameter because it was approximately in the middle of our range of CO values. As we have seen, this is not a critical parameter for temperature calculations. Initially, both CFAST versions were run using our standard OD value of 0.06. This resulted in rather large discrepancies in the predicted upper layer gas temperatures (about 80°C) between the two versions. This was attributed to the fact that CFAST 2.1 used fixed absorbance coefficient values (0.5 m-1 and 0.01 m-1 for upper and lower layers, respectively) whereas

[7] We specify hydrocarbons because the additional parameters HCl, HCN and O2 are important for fuels that contain chlorine, nitrogen or oxidizer.

```
VERSN    3 SHADWELL/688 Laundry compartment
#       Sim.time  Print  Hist.  Disp.  Copies
TIMES     1250      1      3      0      0
#        Temp.    Press.     Elev.
TAMB   285.900   101300.   0.000000
EAMB   286.300   101300.   0.000000
#      Cmpt. 1   Cmpt. 2
#Floor elevation
HI/F   0.00
#X dimen.
DEPTH  1.75
#Y dimen.
WIDTH  6.07
#Z dimen.
HEIGH  2.57
#Materials
CEILI  SHIP3/8
WALLS  SHIPLR
FLOOR  SHIP3/8
#      Cmpt#   Cmpt#   Vent#   Width    Soffit    Sill    Wind
HVENT  1       2       1       0.66     1.90      0.00    0.00
#      Cmpt#   Cmpt#   Vent#    <-Width Fract.->
CVENT  1       2       1        1.00       1.00
#        X     Y     Z
FPOS   0.91  1.83  0.19
#Fire Cmpt
LFBO      1
#Fire Type (1 = unconstrained; 2 = constrained)
LFBT      2
#                t0       t1
FTIME                    1250.
#Mass pyrolysis rate
FMASS          0.0253   0.0229
#       Mol Wt   Rel Hum   LOL        Hc      Init T   Ign. T  Rad. fract.
CHEMI    184.      100.    10.   4.19E+007    285.9     330.     0.30
#H:C mass ratio (fuel composition)
HCR            0.143     0.143
#O:C mass ratio (fuel composition)
O2             0.0       0.0
#Soot:CO2 mass ratio (combustion)
OD             0.06      0.06
#CO:CO2 mass ratio (combustion)
CO             0.056     0.056
#HCN:fuel mass ratio (pyrolysis)
HCN            0.0       0.0
#HCl:fuel mass ratio (pyrolysis)
HCL            0.0       0.0
```

Listing 5. CFAST Input Specification for Modeling the Laundry Room.

The meanings of the keywords are discussed in the text. Lines which begin with the pound sign (#) are comments and are ignored by CFAST.

```
#Toxics:fuel mass ratio (pyrolysis)
CT              0.0       0.0
CJET OFF
DUMPR model.HI
```

Listing 5. CFAST Input Specification for Modeling the Laundry Room (Continued).

version 3.1.4 incorporates an improved absorbance algorithm [4] which calculates absorbance coefficients from the predicted gas composition.

As was mentioned previously, radiation is primarily a cooling mechanism for the upper layer and a heating mechanism for the lower layer and for all surfaces. Therefore, except for the upper layer, energy input may be considered the product of an incident flux and an absorbance factor. Furthermore, the flux term has a fourth power dependence on the upper layer temperature. Due to the large upper layer temperature differences between the two versions, the differences in all other temperatures were due to a convolution of a different flux with a different absorbance, making analysis difficult. Accordingly, the model inputs were modified by reducing the OD to minimize upper layer temperature differences. Thus, any remaining differences in the surface temperatures could reasonably be attributed to factors specific to the surface in question.

Since the absorbance coefficients used in CFAST 2.1 do not correspond exactly to any particular value of OD (the relationship is complex and also involves HCR and CO), we adjusted OD empirically and found that, for an OD of 0.005, a negligible temperature difference (approximately 4 °C) was obtained. Using this input, the differences between temperature predictions for the two versions were calculated, as TCFAST3.1.4 – TCFAST2.1, and are shown in Figure 23.

As seen in the figure, relative to version 2.1, version 3.1.4 predicts that the lower layer temperature will be nearly unchanged, the upper wall and ceiling will be on the order of 75 °C cooler, the lower wall will be about 75 °C hotter and the floor will be approximately 100 °C hotter.

The result for the lower layer gas is reasonable since we have taken great care to make the gas absorbances as similar as possible in the two cases. Considering only absorbance, we would expect the surface temperatures to also be approximately the same in both versions. The fact that they are not is evidence that some factor other than absorbance has been changed within the model. There were many changes between versions 2.1 and 3.1.4 and we have no way to determine which one (or which combination) was responsible for the reduction in surface temperatures.

The most important observation is that the upper wall and the ceiling behave in the same manner. Considering that these two surfaces are exposed to virtually the same conditions, this similarity in behavior is expected. For the same reason, we would expect the floor and lower layer to respond similarly. However, they do not — the floor temperature is found to change by a much larger amount than does the lower wall. This discrepancy leads us to suspect that there is an error in CFAST's floor temperature calculation and that this error is caused by a change that was introduced into the model sometime between version 2.1 and 3.1.4. Unfortunately, since we have no intermediate versions to test, we can not isolate the error any further.

3.3.2 Expected effects of combustion chemistry

In looking more closely into the interactions among the HCR, OD and CO parameters, it must be noted that our purpose is not to make quantitative predictions — that is what CFAST is already doing. Rather, the purpose is to provide an estimation method that may be helpful in identifying

suspicious predictions that should be closely inspected. In particular, we were interested in investigating the behavior of CFAST when the HCR parameter was varied.

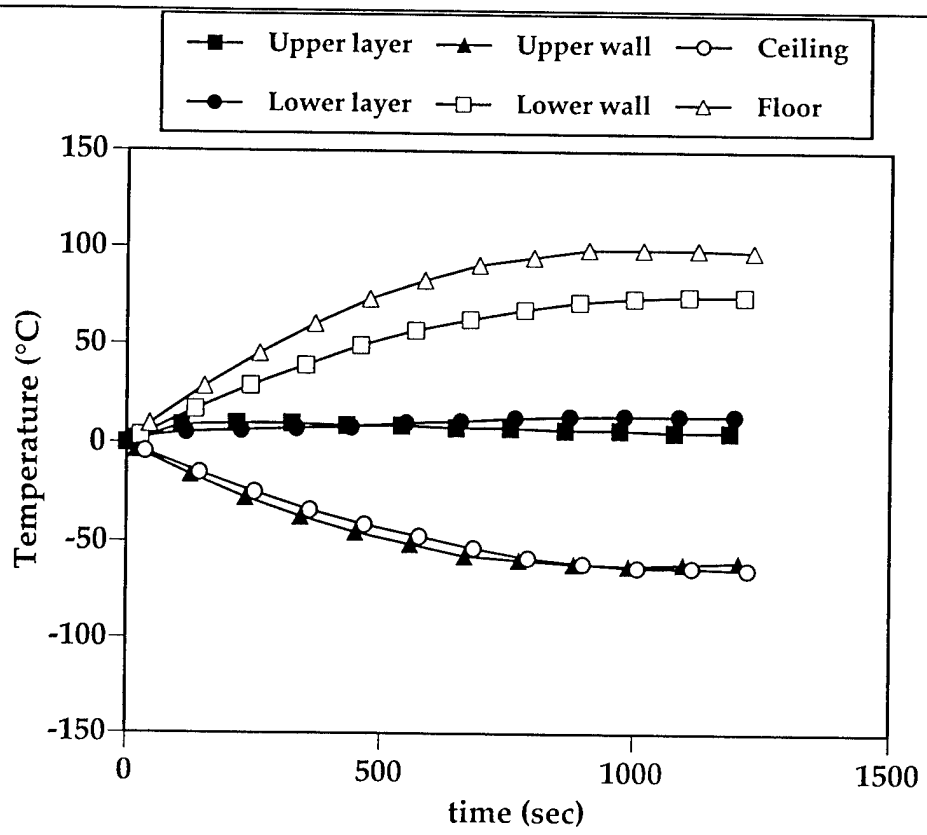

Figure 23. Differences Between CFAST 3.1.4 and CFAST 2.1 Predicted Temperatures

These temperature differences, which were calculated as $T_{CFAST3.1.4} - T_{CFAST2.1}$, illustrate the apparently anomalous behavior of the floor in version 3.1.4.

We start by defining the following symbols:

$m_i \equiv$ mass of species i
$W_i \equiv$ molecular weight of species i
$M_i \equiv$ moles of species i
$m_i^j \equiv$ mass of species i in form j
$K_H \equiv m_H / m_C$ (HCR parameter)
$K_S \equiv m_S / m_{CO2}$ (OD parameter)
$K_{CO} \equiv m_{CO} / m_{CO2}$ (CO parameter)

We have replaced the CFAST parameters HCR, OD and CO with constants of the form K_i in order to avoid confusion between the parameter CO and the species CO.

We assume that the fuel is a pure hydrocarbon, for which

$$d\, m_f = d\,(m_C + m_H) \qquad \text{Eqn. 9}$$

where the subscripts f, C and H represent fuel, carbon and hydrogen, respectively. Using the definition of K_H, we calculate the carbon mass in terms of the fuel mass

$$d\,m_C = d\,m_f / (1 + K_H) \qquad \text{Eqn. 10}$$

and the moles of carbon as

$$d\,M_C = d\,m_f / W_C(1 + K_H) \qquad \text{Eqn. 11}$$

If we assume that the combustion reaction is of the form

$$F + O_2 \longrightarrow S + CO + CO_2 + H_2O$$

where F is fuel and S is soot, then we have the carbon mass balance

$$m_C = m_C^{S} + m_C^{CO} + m_C^{CO2}$$

which, expressed as molar quantities, becomes

$$m_C = nM_SW_C + M_{CO}W_C + M_{CO2}W_C \qquad \text{Eqn. 12}$$

where n, the average number of moles of carbon per mole of soot, is W_S / W_C

If we apply the definitions of K_S and K_{CO}, we can substitute for M_S and M_{CO} in Equation 12 to obtain

$$d\,m_C = d\,[nK_SM_{CO2}\,(W_{CO2} / W_S)\,W_C + K_{CO}M_{CO2}\,(W_{CO2} / W_{CO})\,W_C + M_{CO2}W_C] \qquad \text{Eqn. 13}$$

Equating Equations 10 and 13, solving for $d\,M_{CO2}$ and replacing n gives an estimate for the production of carbon dioxide as a function of the user inputs, K_i, and the mass of fuel burned

$$d\,M_{CO2} / d\,m_f = \left\{ W_C(1 + K_H)\,[(K_SW_{CO2} / W_C) + K_{CO}\,(W_{CO2} / W_{CO}) + 1)] \right\}^{-1} \qquad \text{Eqn. 14}$$

From the definition of K_H, we know that

$$d\,M_H = (K_H / W_H)\,d\,m_C \qquad \text{Eqn. 15}$$

therefore

$$d\,M_{H2O} = 1/2\,(K_H / W_H)\,d\,m_C \qquad \text{Eqn. 16}$$

and, combining Equations 10 and 15, we get an estimate of the water production in terms of the fuel mass

$$d\,M_{H2O} / d\,m_f = K_H / 2\,W_H\,(1 + K_H) \qquad \text{Eqn. 17}$$

Finally, for soot, we have

$$d\,m_S = K_SW_{CO2}\,d\,M_{CO2} \qquad \text{Eqn. 18}$$

Substitution from Equation 14 into Equation 18 gives us an equation for estimating soot production.

$$dm_S / dm_f = K_S W_{CO2} \left\{ W_C (1 + K_H) [K_S (W_{CO2} / W_C) + K_{CO}(W_{CO2} / W_{CO}) + 1] \right\}^{-1} \quad \text{Eqn. 19}$$

Since the "molecular" weight of soot is not well defined, we have chosen to work with mass units for this calculation.

Knowing the mass loss rate, we can now estimate the production rates for the three species that contribute to absorption. We can not calculate actual concentrations because we have no way to account for losses due to mass transport. However, zone models treat layers as being well mixed, so any mass loss process will effect all species equally. Therefore, we can estimate trends in relative concentrations from these equations.

With the gas concentrations from Equations 14 and 17 and the predicted gas temperatures, it is possible to estimate the gas phase absorbances by interpolating the graphs provided in reference [12]. Note that this requires that concentration be converted from moles to partial pressure using the ideal gas law. The soot contribution may be estimated from

$$\alpha_S = 1195.5 \, f_V \, T \quad \text{Eqn. 20}$$

(Equation 6 in reference [4]) where a_S is in units of m^{-1}, f_V is the soot volume fraction and T is the soot temperature (assumed to be in equilibrium with the gas) in kelvins. The volume fraction is calculated from the soot mass and the zone dimensions using 1800 kg/m^3 as a typical soot density.

In general, estimation of temperature effects from relative species concentrations is not practical due to the complexities of absorbance. Fortunately, carbon dioxide and water vapor have similar absorption properties[8] [12], so we may treat them as being approximately equivalent on a molar basis. Soot is a stronger absorber by orders of magnitude so, in most cases, we can reasonably neglect the effects of both gases when soot is present.

With these considerations in mind, we can make rough estimates of the effects of changing some of the CFAST inputs. Table 6 compares the results for two HCR values (0.05 and 0.30) and two values of OD (0.00 and 0.06) with a fixed CO value of 0.056. A lower layer temperature of 398 K was assumed, based on Figure 22, and the volume and path length were 1 m^3 and 1 m, respectively. Because only relative magnitudes are significant, we arbitrarily chose the latter two values to simplify the computations.

Based on this analysis, we see that changing the HCR input can have a larger effect on absorbance when soot is present than when it is absent, which is what we saw in Figure 22. This may be counter-intuitive since our naïve expectation is that soot effects should dominate and, therefore, HCR should have a significant impact only in the absence of soot. This simplistic analysis does not take into account the fact that the OD parameter is normalized to carbon dioxide mass, rather than to fuel mass.

[8] For our purposes, only the wavelength-integrated absorptivity is important. Thus, although the absorbance spectra of water vapor and carbon dioxide are very different, the overall radiation transport effects of a given concentration of either gas is of the same order of magnitude.

			HCR	
			0.05	0.30
OD	0.00	Carbon Dioxide	0.2	0.2
		Water Vapor	0.1	0.5
		Total gas	0.3	0.7
		Soot	0.0	0.0
	0.06	Carbon Dioxide	0.2	0.2
		Water Vapor	0.1	0.5
		Total gas	0.3	0.7
		Soot	42.3	34.0

Table 6. Estimated Relative Absorbance Coefficients for Various HCR and OD.

Species concentrations were calculated from Equations 13, 16 and 18 and the absorbance coefficients (m^{-1}) were estimated from reference [13] (for gas species) and Equation 19 (for soot) using the lower layer temperature from Figure 21. Only the relative magnitudes of the values are meaningful.

4.0 COMPARISON WITH EXPERIMENTAL RESULTS

In the preceding section, we developed the basic fire specification for this simulation and discussed some of the model predictions from the perspective of physical reasonableness and internal consistency. In this section, we compare the model predictions with actual test results.

4.1 Instrument Configuration

In the initial experiment design, the Laundry Room was instrumented with two vertical thermocouple strings, multiple air, deck and bulkhead thermocouples, gas sensors (oxygen, carbon monoxide and carbon dioxide) and optical density meters at three elevations. However, when interior partitions were added to subdivide the compartment into the Laundry Room and Laundry Passageway, the Laundry Room was left with only one thermocouple string, one each of the deck, bulkhead and overhead thermocouples and no optical density instruments. A thermocouple directly above the fire pan provided flame temperatures and served to confirm ignition.

Figure 24 shows the locations of the thermocouple string, flame thermocouple and gas sensors. Unfortunately, the locations of the surface temperature thermocouples were poorly documented. According to the instrumentation plan, the bulkhead thermocouple was located near the port edge of the forward bulkhead of the Laundry Room at an elevation of about 1.5 meters above the deck. The plan indicates that deck and overhead thermocouples were located near the flame thermocouple, approximately one third of the distance between the port and starboard bulkheads. If correct, that would put them below and above the fire pan. The gas sensors were located at an elevation of 0.56 m above the aft edge of the fire pan, approximately aligned with the port edge of the Laundry Room door.

Due to the very limited number of sensors and to the poor choice of location for some, the surface temperatures measurements must be considered to be suspect. In particular, the overhead temperature is expected to be high, due to the location above the fire plume, whereas the deck temperature may be low because the thermocouple was shielded from radiation by the fire pan. The location of the gas inlets suggests that they may have been sampling the fire plume, rather

than the ambient compartment atmosphere. Because of these limitations, the following analysis relies on air temperature data from the thermocouple tree.

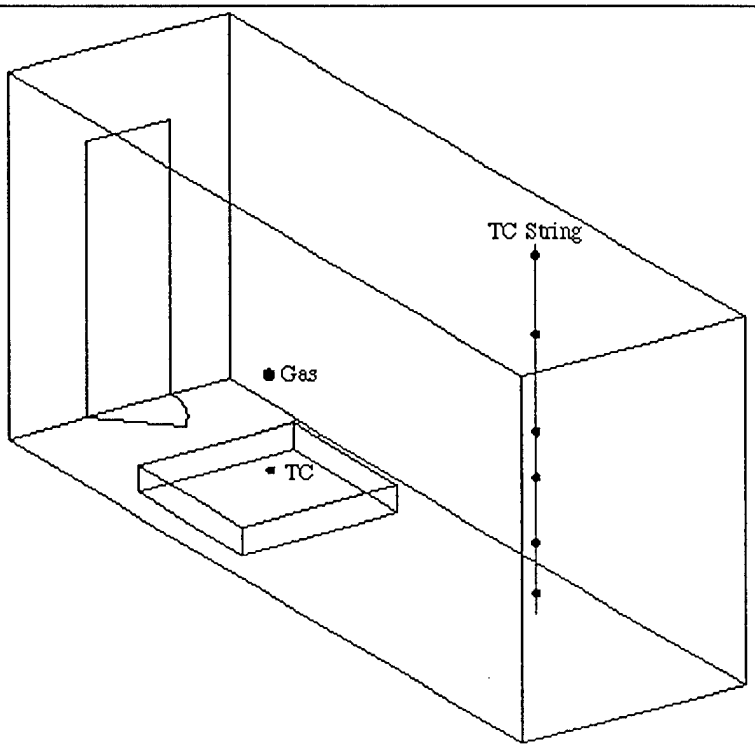

Figure 24. Laundry Room Thermocouples

Air temperatures were measured primarily by a vertical string of type K thermocouples near the forward end of the compartment (TC String). Elevations of the individual thermocouples were: 0.14, 0.50, 0.95, 1.27, 1.94 and 2.50 m above the deck. An additional thermocouple (TC) was located directly above the fire. Gas sensors (Gas) were located above the aft edge of the fire pan at an elevation of 0.56 m.

4.2 Laundry Room Temperatures

Our goal is to compare the measured air temperatures with those predicted by CFAST. However, we must first consider which experimental values correspond to which predictions. Since CFAST is a zone model, the problem is reduced to one of determining which thermocouples were located in the upper layer and which in the lower layer.

The first step is to determine the interface height so that we may assign thermocouples to the proper layer. One approach would be to use the CFAST-predicted interface height. However, doing this implicitly assumes that the model predictions are correct, which is what we are attempting to ascertain. A better way is to estimate the height from the experimental data using a method suggested by Cooper, *et al* [13]. The estimated interface temperature is given by

$$T_i = T_b + 0.15 * (T_t - T_b) \qquad \text{Eqn. 21}$$

where T_b is the bottom (deck level) air temperature and T_t is the top (overhead level) air temperature. Since we do not have air temperatures for deck and overhead levels, we estimate

these by linear extrapolation from the lower two and the upper two thermocouples, respectively. The estimated interface temperature determined from Equation 21 is shown in Figure 25.

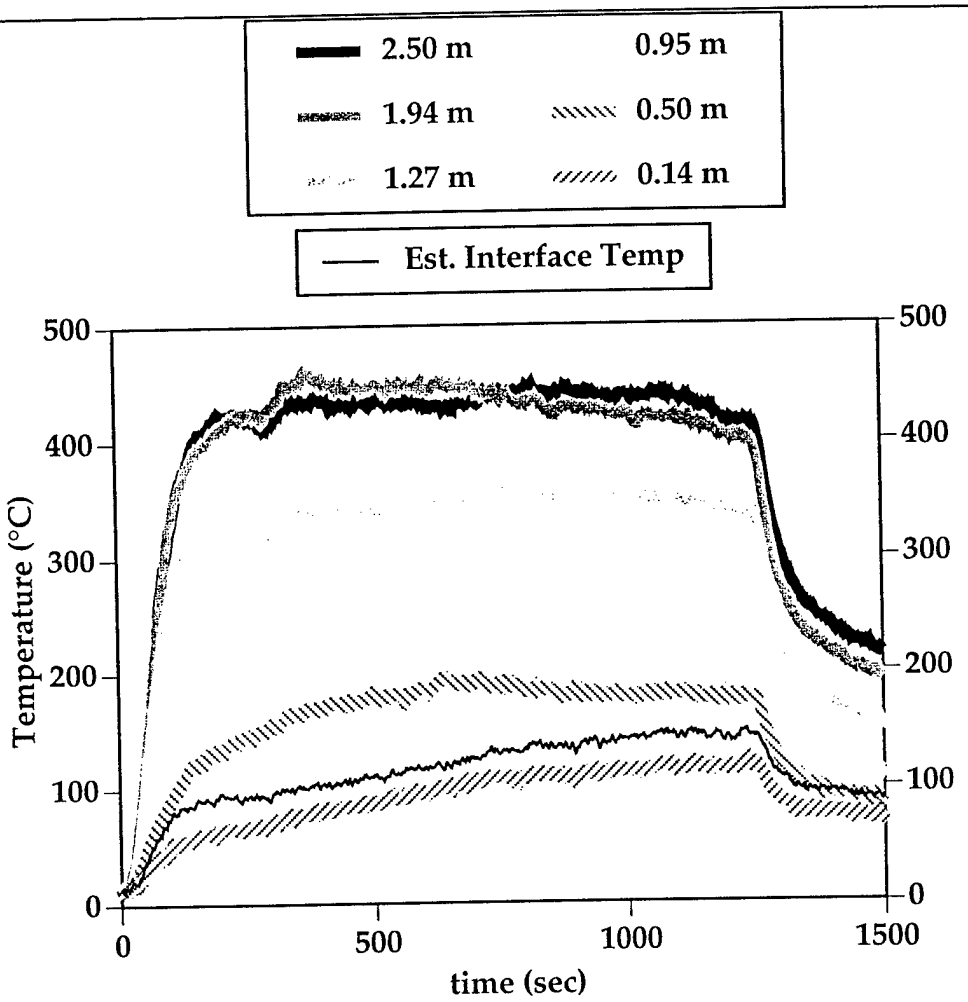

Figure 25. Estimated Interface Temperature

The temperature of the interface between the upper and lower layers was estimated from experimental temperature data using Equation 19.

Once we have calculated an interface temperature, we find the two thermocouples that bracket that temperature (using the extrapolated bottom and top temperatures, if necessary) and perform a linear interpolation between those readings to estimate the interface height. In our case, the estimated interface temperature was consistently between the 0.14 and 0.50 m experimental values and the interpolated interface height (Figure 26) was near 0.3 m for most of the test. During the first seconds after ignition, the differences between temperature readings at different elevations were very small, so our analysis produced some large transients. Once the temperature profile became well established, those artifacts vanished.

The procedure described above is somewhat arbitrary, in that we could as easily have chosen the interface temperature to be something other than 15% of the total deck-to-ceiling temperature difference. In fact, looking at Figure 25, one could argue that this compartment has no interface — there is a relatively smooth gradient from the bottom to (nearly) the top. Equation 21 was used simply because it is a convention.

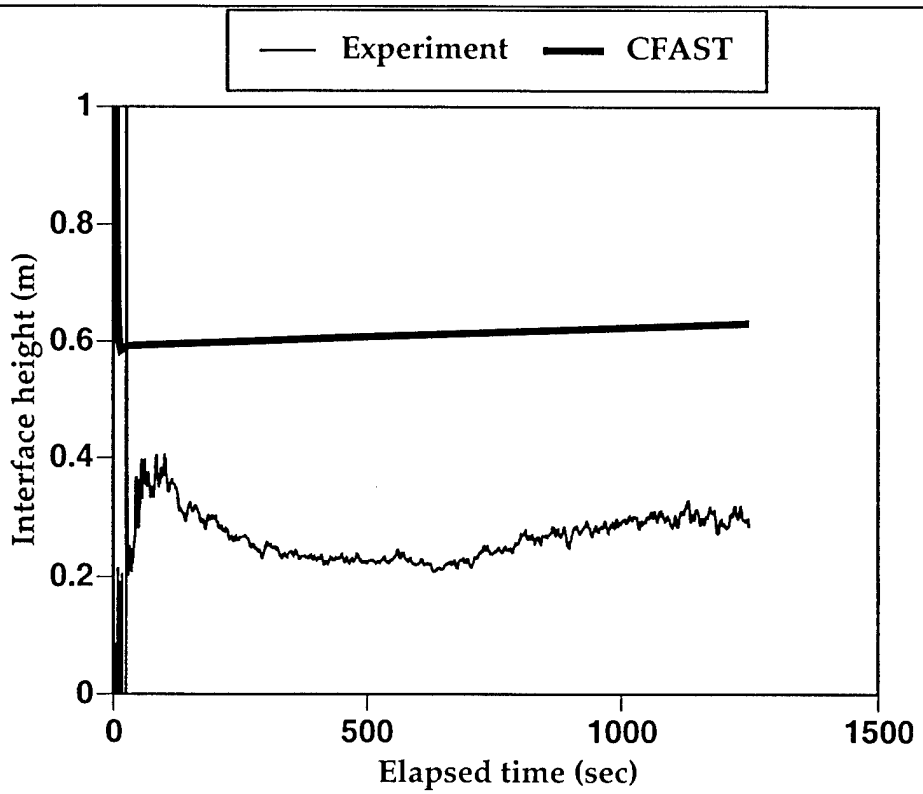

Figure 26. Estimated vs. Predicted Interface Height

The estimated height of the interface was calculated from experimental temperature measurements using the procedure discussed in the text. The spikes near zero time are artifacts due to the small temperature differences between different elevations during the period before the temperature profile becomes well established. The CFAST-predicted interface height is shown for comparison.

Figures 27 and 28, respectively, show the experimental upper and lower temperatures, as calculated using the experimental interface height. Using this method for estimating the interface, there are five thermocouples in the upper layer (at elevations of 0.50, 0.95, 1.27, 1.94 and 2.50 m) and only one in the lower (0.14 m). For the upper layer, we show the mean of those thermocouples and an estimate of the population standard deviation. The latter is calculated by applying Bessel's correction

$$\sigma = [\, n/(n-1)\, s^2]^{1/2} \qquad \text{Eqn. 22}$$

where n is the sample size, s is the sample standard deviation and σ is the estimated population standard deviation.

In Figure 26, we have also shown the CFAST prediction for interface height, which is consistently higher than the value estimated from the experimental data. If the CFAST estimate is correct, then both of the lower two thermocouples should be assigned to the lower layer and the topmost four thermocouples to the upper layer. The upper and lower layer temperatures were recalculated with this distribution of thermocouples and the results are given in Figures 29 and 30.

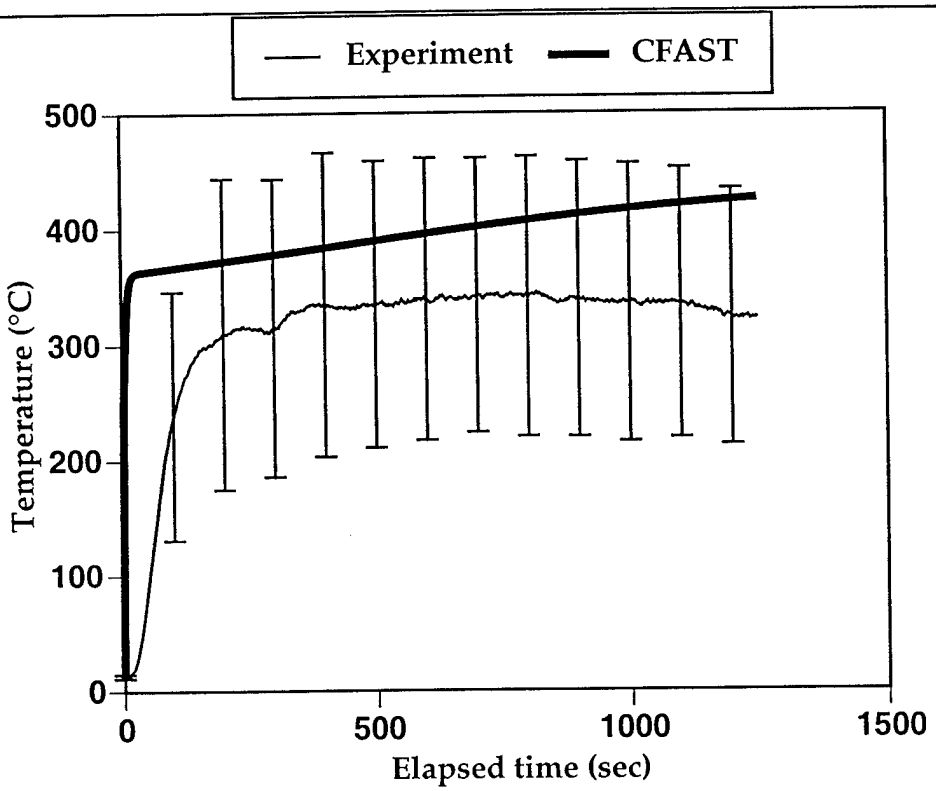

Figure 27. Experimental vs. Predicted Upper Layer Air Temperatures Based on Experimental Estimate of the Interface Height

Using the experimental estimate of the interface height, the upper five thermocouples in the string (0.50, 0.95, 1.27, 1.94 and 2.50 m) were determined to be in the upper layer. The mean of those thermocouples, and the estimated standard deviation of the population, are compared with the CFAST upper layer gas temperature prediction.

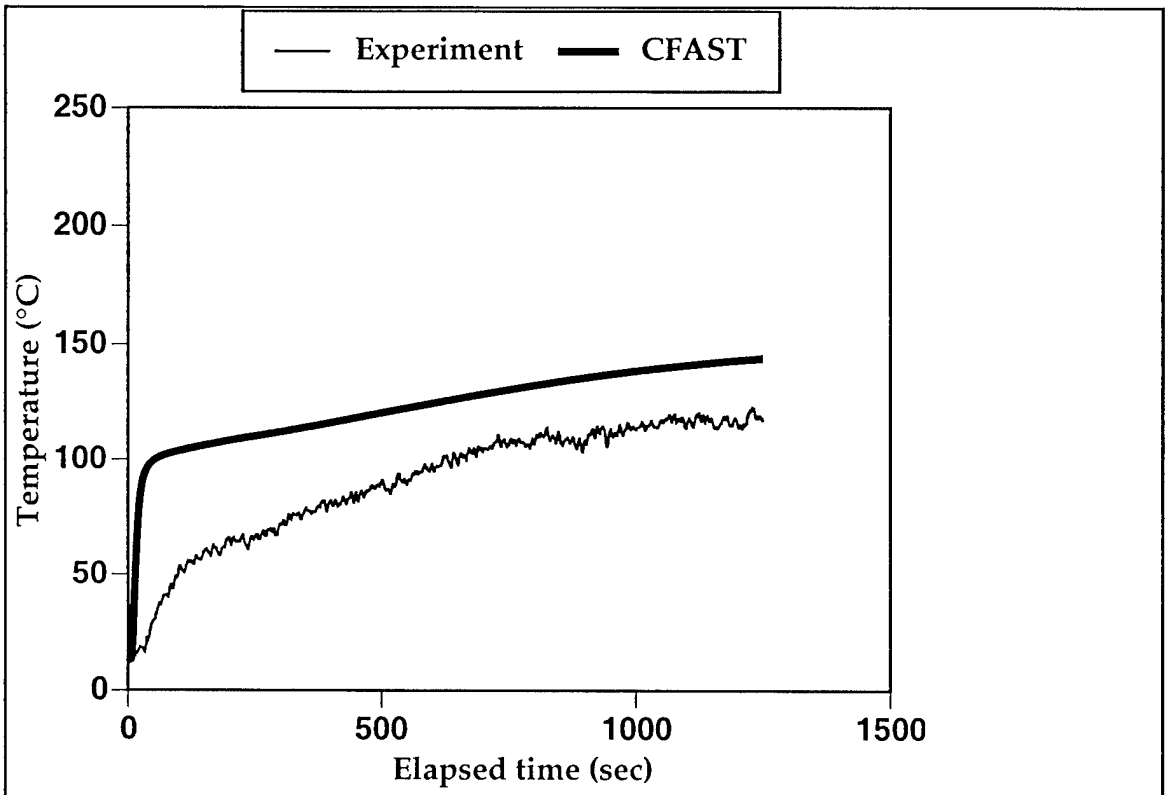

Figure 28. Experimental vs. Predicted Lower Layer Air Temperatures Based on Experimental Estimate of the Interface Height

Using the experimental estimate of the interface height, only the lowermost thermocouple in the string (0.14 m) was found to lie within the lower layer.

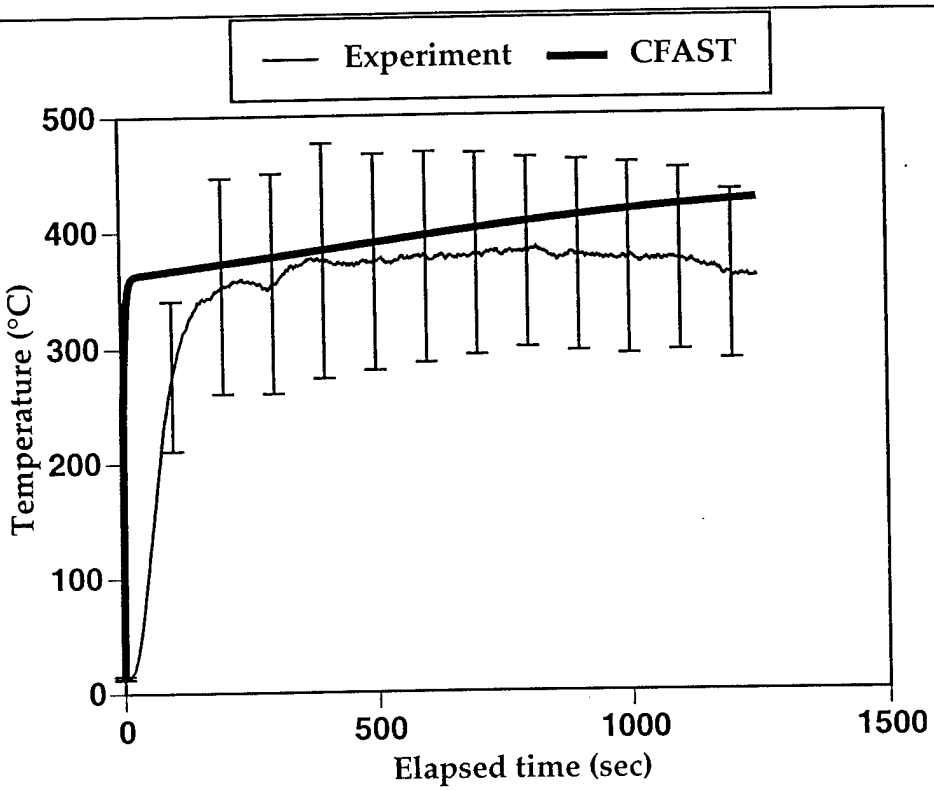

Figure 29. Experimental vs. Predicted Upper Layer Air Temperatures Based on the CFAST-Predicted Interface Height

Using CFAST interface height prediction, the upper four thermocouples in the string (0.95, 1.27, 1.94 and 2.50 m) were determined to be in the upper layer. The mean temperature and the estimated population standard deviation, are compared with the CFAST upper layer gas temperature prediction.

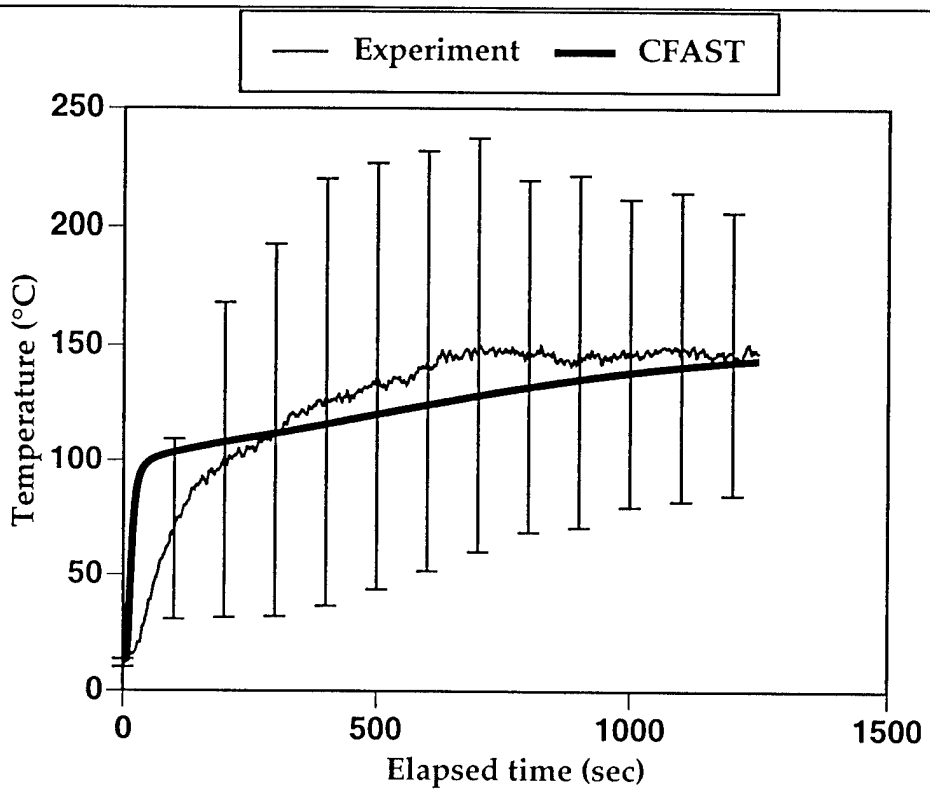

Figure 30. Experimental vs. Predicted Lower Layer Air Temperatures Based on the CFAST-Predicted Interface Height

Using the CFAST prediction for the interface height, the lowermost two thermocouples thermocouple in the string (0.14 m and 0.50) were found to lie within the lower layer. The mean temperature and the estimated standard deviation of the population are compared with the CFAST upper layer gas temperature prediction.

Both methods of estimating the interface height show very good agreement between the experimental values and the CFAST temperature predictions, with the CFAST-predicted interface height yielding a somewhat better fit. In the three cases for which experimental errors may be calculated, we find that the predictions are well within the error bars except for the initial stages of the fire, during which time the model consistently overpredicts the temperatures.

5.0 CONCLUSIONS

Within the Navy, we envision three potential application areas for CFAST: ship design, post-mortem analysis and real-time prediction. The first two of these are immediately feasible but, for real-time prediction to become practical, additional research will be needed. Consideration of this application is beyond the scope of the present project and will not be discussed further.

Our work has concentrated on the development of a CFAST fire specification for a relatively simple, real-world case relevant to the Navy. We have seen that CFAST's input requirements impose some restrictions on what can be modeled and that approximations must sometimes be made to circumvent those limits. Two of the most important of these restrictions, the requirement for a user-specified fire history (heat release rate versus time) and the inability to model combustion chemistry, are closely related. These, and additional limitations, are given in Table 7, along with their possible effects and, for some, suggestions for circumventing the problem.

As we have noted, the heat release rate curve is the single most critical component of the CFAST input file. Unfortunately, heat release rates are highly dependent on the combustion conditions, including such factors as the thermal feedback from the surroundings, the ignitability of secondary fuel sources and the availability of oxygen. The user must somehow estimate, in advance of starting the simulation, the course of the fire growth and decay. For most simulations, this is the most complex part of the user's task.

We have demonstrated that it is feasible to develop such a fire specification almost entirely based on literature values and physically reasonable approximations, with minimal recourse to test results. This is significant because, for applications to both ship design and post-accident investigation, no such data are likely to be available.

Data from SHADWELL/688 tests were used for two purposes in this work. First, experimental mass loss rates provided the basis for the fire specification. As we pointed out, this was necessary because the ultimate goal of this project is to accurately simulate a specific shipboard fire. In the anticipated Naval applications, this level of detail would not be required.

For the ship design application, the general problem of specifying the fire can be addressed by a Monte Carlo approach. With this method, a large number of "typical" shipboard fires would be created by randomly[9] varying the fire size, type and location and, for each such fire, randomly varying vent closures and other factors. The goal would be to estimate the probability of the occurrence of specified levels of damage. Assuming that realistic ranges of fire parameters were selected (perhaps based on historical fire loss data) and that the modeling protocol was statistically valid, designers should be able to produce reliable generalizations regarding fire safety of a proposed ship design, based on CFAST modeling.

In the case of post-mortem analysis, there is often an abundance of information available regarding the site of origin of the fire, the type and amount of fuel, the configuration of the ventilation system and other variables. Also, forensic investigations can frequently provide useful information regarding the spread of the fire — estimates of the temperatures attained, the

[9] Note that the range of variation can be restricted to something that is reasonable. For example, when modeling berthing space fires, it probably is unreasonable to assume a large pool fire.

time of breakthrough into other rooms, and similar factors. With this information in hand, it is quite feasible to simulate the actual events, although some trial and error will likely be needed. In some ways, the present work is similar, except that we have the luxury of actual fire data, rather than forensic reconstructions, for guidance.

Limitation	Effects	Solution
Only one internal ambient state is permitted.	May lead to minor errors in predictions if there are large initial temperature differences among the compartments.	Significance depends on the details of the scenario being modeled.
Compartments must be rectilinear parallelepipeds.	Heat transfer via conduction and radiation will not be correct for surfaces which are not rectangular.	Subject of the next phase of this project.
Ceiling, floor and walls are each limited to a single set of thermophysical properties.	Approximations must be made if the ceiling, floor or walls are composed of multiple regions having different properties.	Area-weighted mean properties were used where necessary.
Compartments have only one, wrap-around wall.	May lead to significant errors if there are large differences in the properties of walls.	No work-around known. A sensitivity analysis is suggested.
User-specified fire histories are required.	The user must know (or be able to accurately estimate), in advance, the development of the fire.	A self-consistent fire algorithm is needed for real-time applications. For design, a sensitivity analysis is suggested
CFAST does not account for the variability of fire chemistry with pyrolysis and combustion conditions.	Predictions of pyrolysis and combustion product concentrations may be incorrect.	Development of correlation functions for fire chemistry is suggested.Use a CFD model if concentrations are critical.

Table 7. Limitations of CFAST.

The primary limitations that we encountered during development of the fire specification, along with typical effects that may be expected, are shown in this table. We have also provided suggestions for circumventing some of the limits.

The second application of actual test measurements was related to the selection of the CO parameter. As we noted, CO is not critical, except for prediction of carbon monoxide concentrations. The value we derived from test data lies near the middle of the range of "reasonable" values that were suggested in reference [11]. In any case, this parameter is highly dependent on the details of combustion so, if accurate carbon monoxide values are required, a field model should be use in preference to CFAST. If only general predictions are needed (for

hazard analysis, for example), simulations should be run with a range of input parameters, as was done in this work.

By comparing the results of our simulation with measured gas temperatures from SHADWELL/688 tests, we have demonstrated that CFAST is capable of reproducing the temperature history of a large-scale shipboard fire with reasonable accuracy without recourse to *ad hoc* adjustment of the model input parameters.

These comparisons required that the thermocouples be partitioned between the upper and lower layers. Two possible methods of accomplishing this partitioning were investigated and it was found that a method based solely on the use of CFAST-predicted interface heights produced slightly better results than an alternate method that requires the use of experimental data. This is fortunate because, for the Navy's intended uses, experimental data are unlikely to be available.

We have also identified several areas in which improvements to CFAST could significantly simplify the process of applying the model to Naval fire problems. We suggest that the use of a fuel database, analogous to the existing materials properties database, would be very useful. It is envisioned that this database would include values for all fuel-related parameters (*e.g.*, molecular weight, heat of combustion and HCR). It could also include appropriate defaults for parameters related to combustion (for example, the default OD might be different for diesel-type fuels than for simple alkanes, such as methane or propane).

A second area for improvement is the parameterization of the combustion process. It may be possible to develop, either empirically or through detailed theoretical modeling, correlation functions relating the production of carbon monoxide and soot to the oxygen to fuel ratio. If successful, this would eliminate the need for user-defined OD and CO values which, as we have seen, are the most difficult parameters to assign *a priori*.

As part of this "Analysis of the CFAST Fire Model Operating Envelope" task, further work is now in progress to address questions related to the application of CFAST to more complex geometries.

6.0 ACKNOWLEDGMENTS

The work described in this report was performed by the Chemistry Division of the Materials Science and Component Technology Directorate, Naval Research Laboratory. The work was funded by the Office of Naval Research, Code 334, under the Damage Control Task of the FY99 Surface Ship Hull, Mechanical, and Electrical Technology Program (PE0602121N).

The authors wish to thank Jean Bailey (NRL Code 6183) for her assistance in performing the CFAST modeling and Brad Williams (NRL Code 6185) for his helpful comments regarding this manuscript.

7.0 REFERENCES

1. "CFAST, the Consolidated Model of Fire Growth and Smoke Transport", Richard D. Peacock, Glenn P. Forney, Paul Reneke, Rebecca Portier and Walter Jones, US Department of Commerce Technical Report TN 1299, 1993.

2. "Validation of Fire/Smoke Spread Model (CFAST) Using ex-USS SHADWELL Smoke Ejection System Fire Tests", Jean L. Bailey, NRL Ltr Report 6180/0007, 1994.

3. "Validation of Fire/Smoke Spread Model (CFAST) Using Ex-SHADWELL Internal Ship Conflagration Control (ISCC) Fire Tests", J. L. Bailey and P. A. Tatem, NRL Memo Report NRL/MR/6180--95-7781, 1995.

4. "An Improved Radiation Transport Submodel for CFAST", John B. Hoover, Jean L. Bailey and Patricia A. Tatem, Combust. Sci. and Tech., **127,** 213-229 (1997).

5. "Meta-Analysis of Data from the Submarine Ventilation Doctrine Test Program", J. B. Hoover, P. A. Tatem and F. W. Williams, NRL Memo Report NRL/MR/6180--98-8168, 1998.

6. "A User's Guide to FAST: Engineering Tools for Estimating Fire Growth and Smoke Transport", Richard D. Peacock, Paul A. Reneke, Walter W. Jones, Richard W. Bukowski and Glenn P. Forney, US Department of Commerce Special Report 921, 1997.

7. "Heat Release Rate: The Single Most Important Variable in Fire Hazard", Vytenis Babrauskas and Richard D. Peacock, Fire Safety Journal, **18**, 255 (1992).

8. "Characteristics of Large Diffusion Flames Burning in a Vitiated Atmosphere", J.H. Morehart, E.E. Zukoski and T. Kubota, Third International Symposium on Fire Safety Science, Edinburgh, p. 575, 1991.

9. "Introduction to Combustion Phenomena", A. Murty Kanury, Gordon and Breach, N.Y., p 144, 1975.

10. "Standard Specification for Diesel Fuel Oils," ASTM Specification D975-98a, in "1999 Annual Book of ASTM Standards, Section 5, Petroleum Products, Lubricants and Fossil Fuels," ASTM, W. Cohshohocken, PA, **05.01**, 340, 1999.

11. "Military Specification: Fuel, Naval Distillate," MIL-F-16884J, Naval Sea Systems Command, Washington, DC, p. 6, 1995.

12. SFPE Handbook, 1st Ed., p. 1-221 - 1-222.

13. "Radiation Properties of Gases," D.K. Edwards, in "Handbook of Heat Transfer Fundamentals", W.M. Rohsenow, J.P. Hartnett and E.N. Ganic, Eds., McGraw-Hill, N.Y., p.14-74 & 14-75, 1985.

14 "An Experimental Study of Upper Hot Layer Stratification in Full-Scale Multiroom Fire Scenarios," L.Y. Cooper, M. Harkleroad, J. Quintiere and W. Rinkinen, J. Heat Transfer, **104**, 741 (1982).

Appendix A

CFAST Keywords Used in Modeling of the Submarine Ventilation Doctrine Configuration

VERSN	Version of CFAST for which the input file is intended. A title may also be specified for identification purposes.
TIMES	Simulation time and frequency of on-screen and file outputs.
DUMPR	Name of output file to be used.
RESTR	Name of restart fire, if any.
FTIME	Event timeline.

Table A-1. Simulation Control Keywords

TAMB	Internal ambient temperature, pressure and reference elevation.
EAMB	External ambient temperature, pressure and reference elevation.

Table A-2. Ambient Environment Keywords

DEPTH	Depth (x-dimension) of the compartments, in meters. See FPOS.
WIDTH	Width (y-dimension) of the compartments, in meters. See FPOS.
HEIGH	Height (z-dimension) of the compartments, in meters. See FPOS.
HI/F	Floor elevation, relative to the reference elevation, in meters.
CEILI	Reference to an entry in the thermophysical properties database describing the ceilings.
WALLS	Reference to an entry in the thermophysical properties database describing the walls.
FLOOR	Reference to an entry in the thermophysical properties database describing the floors.
THRMF	Name of the thermophysical database to be used. If not specified, a default database, THERMAL.DF, is used.
HVENT	Definition of a horizontal vent, including the source and sink compartments, the vent number within the source compartment, the vent width and the heights of the soffit and sill.
VVENT	Definition of a vertical vent, including the source and sink compartments, the vent area and the shape (either round or square).
CVENT	Opening (width) of a horizontal vent as a fraction of the maximum width specified by the corresponding HVENT line.
CFCON	Enables vertical heat conduction through a ceiling to the floor of the compartment above.

Table A-3. Model Geometry Keywords

LFBO	Compartment number in which the main fire is located
FPOS	Coordinates (right-handed, Cartesian) of the fire location within the compartment relative to the lower, left, rear corner.
LFBT	Fire type. Type 1 is unconstrained by oxygen availability; type 2 is constrained.
FQDOT	Heat release rate of the burning fuel at the times specified by FTIME.
FMASS	Mass loss (pyrolysis) rate of the fuel at the times specified by FTIME
CHEMI	Miscellaneous parameters related to fuel combustion chemistry. Includes molecular weight and heat of combustion.
HCR	The mass ratio of hydrogen to carbon in the fuel.
O2	The mass ratio of available oxygen in the fuel to the total mass of fuel. This applies only to special cases, such as rocket fuels, in which the fuel consists of a mixture of oxidizing and reducing agents.
HC	Ratio of the mass of HCN produced by pyrolysis to the mass of fuel pyrolyzed.
HCL	Ratio of the mass of HCl produced by pyrolysis to the mass of fuel pyrolyzed.
CT	Ratio of the mass of a virtual "total toxics" product to the mass of fuel pyrolyzed. This product is taken to be representative of the combined toxic effects of the actual pyrolysis and combustion products.
OD	Mass ratio of soot to carbon dioxide in the combustion products. This parameter is very important for correct prediction of temperatures (reference [4]).
CO	Mass ratio of carbon monoxide to carbon dioxide in the combustion products.
FHIGH	Height of the base of the fire (above the reference position established by FPOS) at the times specified by FTIME.
FAREA	Horizontal area of the base of the fire at the times specified by FTIME.
CJET	Switches between the "standard" and "ceiling jet" model of convective heat transfer to the ceiling.

Table A-4. Fire Description Keywords